Results in Engineering 28 (2025) 107237

Contents lists available at ScienceDirect

Results in Engineering

journal homepage: www.sciencedirect.com/journal/results-in-engineering

Research paper

Harnessing geothermal energy in Kazakhstan: Techno-economic assessment of Organic Rankine Cycle application in the Almaty region

Nazym Abdlakhatova [a,c,e,*], Luis Frölén Ribeiro [b,e], Larysa Savosh [b,f], Seitzhan Orynbayev [c], Amanzhol Tokmoldayev [d], Talgat Zhussip [a]

[a] Kazakh National University of Water Management and Irrigation, 080000 Taraz, Kazakhstan
[b] Instituto Politécnico de Bragança, 5300-253, Bragança, Portugal
[c] Taraz University named after M. Kh. Dulaty, 080000 Taraz, Kazakhstan
[d] Kazakh National Agrarian Research University, 050000 Almaty, Kazakhstan
[e] GICoS, Instituto Politécnico de Bragança, 5300-253, Bragança, Portugal
[f] Lutsk National Technical University, Lutsk - Ukraine

ARTICLE INFO

Keywords:
Kazakhstan
Geothermal resources
Organic Rankine Cycle (ORC)
Geothermal power
Almaty

ABSTRACT

This study assesses the feasibility of geothermal electricity generation in Kazakhstan using Organic Rankine Cycle (ORC) systems to exploit low- to medium-temperature geothermal resources. ORC systems efficiently convert heat from moderate-temperature sources into electricity using organic fluids with boiling points lower than that of water. Globally, ORC systems contribute over 3 GW of installed capacity, accounting for 25.1 % of geothermal power production. Kazakhstan's electricity generation rose from 85.3 TWh in 2013 to 98.4 TWh in 2023, with associated CO_2 emissions increasing from 67.4 to 77.0 million tonnes. Despite known geothermal reserves, the country has not yet developed geothermal power capacity. This study identifies the geothermal potential of the Mangystau-Ustyurt and Almaty Artesian basins, with a focus on the Zharkent field. Among the wells evaluated, Well 5539, with a wellhead temperature of 103 °C, is estimated to generate 5.467 TWh of electricity annually, accounting for 51.9 % of the regional potential. Wells 1-RT and 2-TP also show strong promise, with annual outputs of 2.471 and 2.598 TWh, respectively. Thermal power availability ranges from 5.1 to 8.3 MW, and the combined yearly potential of 10.5 TWh could offset 82.1 % of the Almaty region's electricity deficit and avoid 5.47 million tonnes of CO_2 emissions annually. The methodology includes thermodynamic modelling and well data analysis to estimate geothermal electricity potential. This study represents the first assessment of ORC-based geothermal power in Kazakhstan for low-temperature wells in a specific region.

1. Introduction

Geothermal energy can be harnessed in two primary ways: for direct heat use and electricity generation. Direct applications involve extracting heat from the Earth for residential heating, greenhouses, and industrial processes—widely implemented in geothermal-rich regions due to their proven efficiency and simplicity. In contrast, electricity generation typically relies on high-temperature geothermal reservoirs. A key innovation for lower-temperature resources is the Organic Rankine Cycle (ORC) system, which uses an organic fluid with a lower boiling point than water to convert geothermal heat into electricity. This system enables the exploitation of geothermal sources previously deemed unsuitable for power generation.

ORC systems currently account for >3 GW of installed geothermal power capacity worldwide, comprising approximately 25.1 % of the total, especially in low- to medium-temperature fields [1]. Their deployment demonstrates the technology's maturity and scalability.

In June 2023, the International Energy Agency (IEA) hosted its 8th Annual Global Conference on Energy Efficiency in Versailles, France. The resulting Versailles Statement, endorsed by 46 countries, called for a doubling of global energy efficiency progress by 2030 to support sustainable growth and achieve net-zero emissions by 2050 [2,3]. Notably, Kazakhstan was not among the signatories, reflecting its current misalignment with international commitments to energy transition and efficiency. Despite possessing substantial geothermal resources, ORC-based geothermal electricity generation remains absent from

* Corresponding author.
E-mail address: an060885@gmail.com (N. Abdlakhatova).

https://doi.org/10.1016/j.rineng.2025.107237
Received 27 May 2025; Received in revised form 1 September 2025; Accepted 10 September 2025
Available online 11 September 2025

national energy planning Table 1.

Electricity production in Kazakhstan increased significantly between 2013 and 2023, rising from 85.323 TWh to 98.389 TWh, an average annual increase of approximately 1.570 GWh. During this period, the share of electricity generated from natural gas grew steadily, reaching an average of 10.6 %, while coal continued to dominate the energy mix. This modest shift toward gas reflects a gradual transition, yet the prevailing reliance on coal continues to drive environmental pressures. CO_2 emissions from the power sector rose from 67.424 million tonnes in 2013 to 77.042 million tonnes in 2023, with an average annual increase of 1.16 million tonnes—figures derived from the fossil fuel breakdown of operating thermal power plants [4,5].

As of January 1, 2024, Kazakhstan's installed electricity capacity is composed of 66.7 % coal, 21.5 % gas, 7.3 % hydro, and 4.5 % other renewables [6]. The country currently hosts 130 renewable energy facilities, with a combined installed capacity of 2388.3 MW (Table 2). However, when compared to Kazakhstan's total electricity consumption—which exceeded 115 TWh in 2023 [7]—this renewable capacity remains modest. Even under optimal conditions, it would generate approximately 20.9 TWh per year, accounting for <20 % of national demand. This discrepancy highlights Kazakhstan's continued reliance on fossil fuels and underscores the need to accelerate the development of renewable infrastructure. While the current trajectory signals progress, the pace of expansion remains insufficient to meet the country's decarbonisation goals.

This study serves as a preliminary assessment of the feasibility of geothermal electricity generation in Kazakhstan. By integrating geothermal sources into the national energy mix, the country could enhance energy diversification, decentralise generation, strengthen energy security, and make a meaningful contribution to its sustainable development goals.

1.1. State-of-the-art Kazakhstan's geothermal potential

Kazakhstan possesses extensive geothermal resources, yet these remain vastly underutilised and are currently restricted to low-enthalpy applications, such as spas, baths, greenhouse heating, and space heating. Despite this, the country has significant untapped potential for electricity generation, particularly through the application of Organic Rankine Cycle (ORC) systems to low- and medium-temperature geothermal sources. Exploiting this potential could deliver considerable local and national benefits, enhance energy security, and support the country's transition toward a more decentralised and diversified renewable energy portfolio.

Globally, ORC technology is well established and currently accounts for over 3 GW of installed geothermal capacity, representing approximately 25.1 % of the total [1]. However, in Kazakhstan, scholarly and policy attention has remained focused almost exclusively on direct-use geothermal applications [8–10]. Electricity generation via geothermal energy has yet to be systematically studied or integrated into national energy planning. There is a notable absence of system-level assessments that consider the feasibility of ORC implementation under local conditions, such as well characteristics, infrastructure constraints, electricity pricing, and regulatory frameworks. This study addresses that critical gap by presenting the first techno-economic evaluation of geothermal electricity production in Kazakhstan using ORC systems.

Table 1
A decade of thermal power electrical production in Kazakhstan [4,5].

Year	Electricity production by coal (GWh)	Electricity production by gas (GWh)	Total electricity production (GWh)	Total CO_2 emissions (Mt CO_2)
2013	77,622	7701	85,323	67.424
2014	78,773	8236	87,009	68.629
2015	81,371	7280	88,651	70.291
2016	82,110	7408	89,518	70.960
2017	82,425	8373	90,797	71.691
2018	86,795	9119	95,914	75.640
2019	85,955	8976	94,931	74.881
2020	86,663	9528	96,190	75.732
2021	91,164	10,702	101,866	79.999
2022	88,622	10,942	99,564	78.032
2023	87,366	11,023	98,389	77.042

Table 2
The Renewable power available in Kazakhstan [6].

Technology	Number of facilities	Nominal Power (MW)
Windpower	46	957.5
Photovoltaic	44	1149.0
Hydropower	37	280.0
Biomass	3	1.8
Total	130	2388.3

Historically, the most comprehensive geothermal studies were conducted during the Soviet period, particularly between 1982 and 1991, in southern Kazakhstan. These involved prospecting and appraisal work in regions such as Turkestan, Arys, and Almaty, confirming substantial geothermal reserves suitable for space heating and domestic hot water supply. A 2022 pre-feasibility study further corroborated the long-standing recognition of this potential [11].

Geothermal waters are widespread throughout Kazakhstan due to the presence of deep artesian basins with water-bearing formations. >100 exploration wells have revealed thermal waters with favourable characteristics—adequate flow rates, temperatures, and chemical profiles—for energy use. There are currently 3544 registered underground water deposits, collectively yielding over 42 million cubic metres per day. These reserves are naturally replenished through precipitation and surface runoff [12], offering long-term sustainability.

Despite this promising profile, groundwater in Kazakhstan and the broader Central Asian region remains predominantly reserved for drinking purposes, and its energy potential remains underexploited. Unlocking this potential would support national decarbonisation objectives, reduce reliance on fossil fuels, and open opportunities for rural electrification and industrial applications. To spatially characterise geothermal potential, this study created the first territorial geothermal distribution map of Kazakhstan using QGIS 3.32.0, based on the national geothermal source registry [13].

As illustrated in Fig. 1 and Table 3, geothermal sources in Kazakhstan are geographically diverse and stratified by temperature, as determined through spatial analysis conducted in QGIS using cartographic data from the National Atlas of the Republic of Kazakhstan [13]:

- Low-temperature sources (20–40 °C), marked in green, cover approximately 14 % of the national territory and are concentrated in North Kazakhstan, Pavlodar, East Kazakhstan, Zhambyl, Kyzylorda, and West Kazakhstan.
- Moderate-temperature sources (40–75 °C), shown in yellow, cover 18 % of the area, primarily located in Pavlodar, Zhambyl, Kyzylorda, Mangystau, and West Kazakhstan.
- High-temperature sources (75–100 °C), marked in brown, are located in Mangystau, Atyrau, and Turkistan, covering around 5 % of the territory.
- Very high-temperature sources (>100 °C), shown in crimson, are located in the Almaty and Mangystau regions, accounting for approximately 2 % of the national area.

These sources are currently used for heating, greenhouses, and bathing purposes but not for power generation. Given that over 85 % of Kazakhstan's electricity is produced from coal-fired thermal plants [12], geothermal electricity offers a low-carbon alternative that is both decentralised and domestically secure.

The reliable assessment of geothermal resources is essential for their sustainable development. Various methods are used to estimate

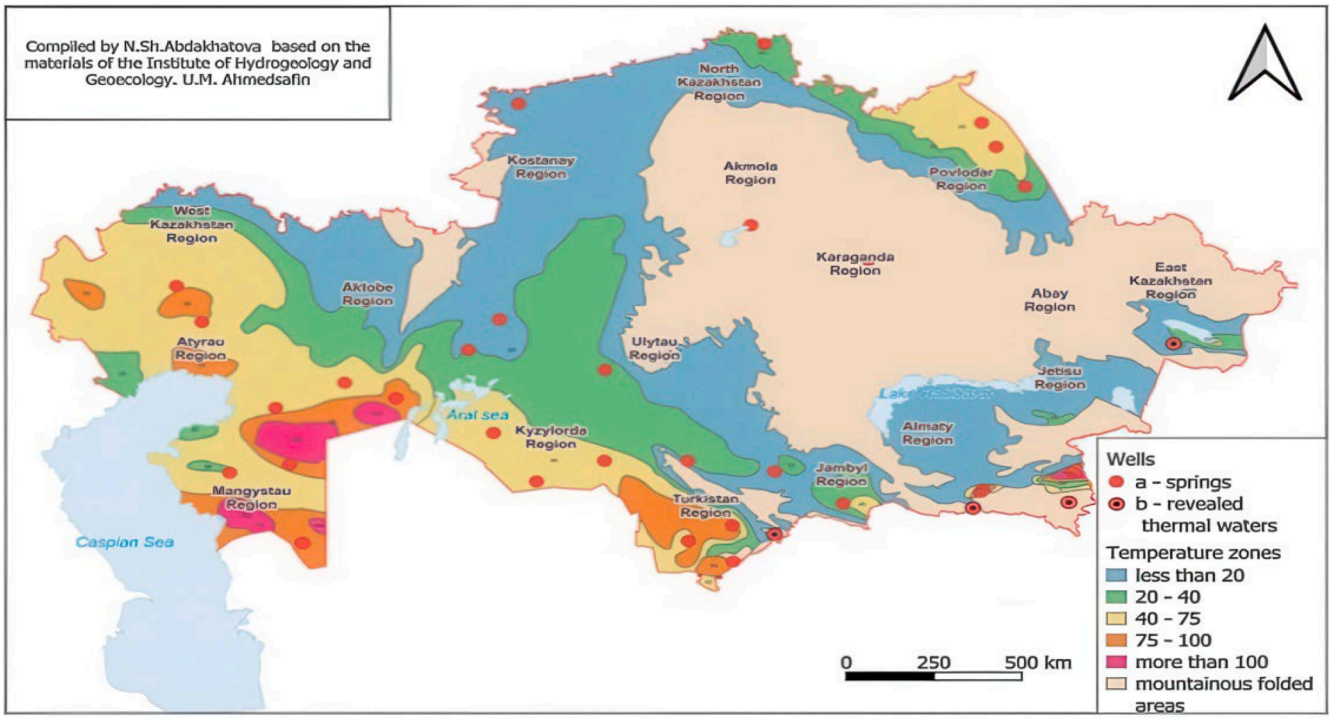

Fig. 1. Map of the distribution of geothermal groundwater in Kazakhstan.

Table 3
Distribution of geothermal sources over the territory of Kazakhstan [13].

ΔT (°C)	Area (%)
20–40	14
40–75	18
75–100	5
>100	2

geothermal potential, including the volumetric method, direct heat extraction method, surface heat flux analysis, magmatic heat budget, planar fault method, power density estimation, decline curve analysis, and numerical modelling [14]. The volumetric method is widely applied for resource quantification and was selected here due to its proven relevance in similar geological contexts, such as Turkey's Gediz graben [15]. For long-term resource management, numerical modelling remains the most effective approach.

In this context, we present the first comprehensive thermodynamic and techno-economic model of a binary Organic Rankine Cycle (ORC) system tailored to Kazakhstan's geothermal conditions. Six geothermal wells were initially evaluated, with three selected for detailed analysis. Among these, Well No 5539 in the Almaty region was chosen as the primary case study due to its favourable thermal output and regional relevance. A comparative analysis of working fluids was conducted, explicitly accounting for the seasonal temperature fluctuations characteristic of the continental climate in Zharkent. This modelling framework provides a robust basis for evaluating the technical feasibility and optimisation of geothermal electricity generation under Kazakhstan-specific constraints.

For the first time, a geothermal power study in Kazakhstan integrates site-specific geothermal well data with system-level thermodynamic modelling and environmental performance indicators. Although the efficiency of ORC systems for low-temperature geothermal resources is well established internationally, their application has not yet been systematically adapted to the geological, climatic, and regulatory context of Kazakhstan. This study begins to fill that gap, addressing a critical deficiency in both the academic literature and national energy planning.

The analysis also provides key insights into how low-enthalpy geothermal systems can serve regions underserved by centralised power infrastructure. Focusing on the Almaty region—Kazakhstan's most populous urban centre, with approximately two million inhabitants—the results demonstrate the potential of decentralised geothermal electricity to reduce regional energy deficits and CO_2 emissions. In doing so, the study contributes not only to the diversification of Kazakhstan's national energy mix but also to the country's alignment with global Sustainable Development Goals.

The novelty of this research lies in its integrated and multi-layered approach. It combines the first spatial screening of geothermal potential across Kazakhstan with the technical characterisation of promising wells, culminating in a detailed assessment of Well No 5539. A simplified yet representative thermodynamic model was developed to estimate energy outputs, and the performance of the ORC system was tested using fourteen different organic working fluids. Technical outputs, including net electric power generation and annual energy production, were quantified and subjected to uncertainty analysis using Monte Carlo simulations. This analysis was followed by a techno-economic evaluation based on the Levelised Cost of Electricity (LCOE) under both deterministic and stochastic production scenarios. Taken together, these contributions provide the first system-level techno-economic characterisation of Kazakhstan's geothermal electricity potential, establishing a scientifically grounded platform for future development, investment, and policy action.

Unlike previous studies, which have focused solely on the direct thermal applications of geothermal resources, such as space heating [16], this study provides the first comprehensive, system-level assessment of electricity generation using ORC technology in the context of Kazakhstan.

2. Materials and methods

2.1. Research area

To generate electrical energy, sources with high temperatures are

needed. Therefore, this study considers in more detail the areas of groundwater occurrence with high temperatures and their chemical composition.

2.1.1. Sources with temperature (75–100 °C)

The Mangystau region has significant industrial reserves of thermal waters with a constant temperature of 60–90 °C in summer and winter, which can form alternative sources of heat and electricity. With its high geothermal potential, this region can provide residents with environmentally friendly and affordable thermal energy, contributing to the decentralisation of energy production. The Mangystau region borders two other areas of Kazakhstan, Atyrau and Aktobe, and two foreign countries, Turkmenistan and Uzbekistan, covering an area of 165.42 km^2. Fig. 2 depicts the temperature zones within the region. In this region, 21 % of the area has a temperature zone of >100 °C, 34 % has a temperature zone of 75–100 °C, 37 % has a temperature zone of 40–75 °C, and 8 % has a temperature zone of 20–40 °C.

Given its high geothermal gradient, industrial relevance, and availability of thermal water resources with stable year-round temperatures, the Mangystau region represents a top-priority candidate for geothermal exploration in Kazakhstan [17,18]. These factors make the area particularly favourable for the deployment of geothermal power systems based on the Organic Rankine Cycle (ORC).

The Mangystau-Ustyurt system of artesian basins in the Aral-Caspian watershed offers significant geothermal potential. The Cretaceous and Jurassic formations are sources of hydrogeothermal resources, with thermal waters containing industrially significant concentrations of iodine, boron, bromine, and other essential micro-components. The well flow rates vary between 140 and 3500 m^3/day, and water mineralisation ranges from 1 to 100 g/dm^3, predominantly sodium chloride. Reservoir temperatures range from 50 to 150 °C, indicating substantial potential for sustainable energy production.

The Almaty Artesian basin, in the western part of the Ili Depression, also shows significant geothermal potential. Neogene and Paleogene thermocautery complexes have been discovered within this area, with depths of up to

2600 m. The water discharged from the springs ranges from 10 to 2200 m^3/day, with mineralisation levels from 3 to 15 g/dm^3. The water temperature at depths of 700–3000 m can reach up to 84 °C. The Zharkent deposit, on the border between the Almaty region and China, covers 8616 km^2, with geothermal sources reaching temperatures up to 165 °C at depth.

2.1.2. Unlocking geothermal potential for power generation

Given the high temperatures and flow rates of geothermal waters, the Zharkent and Mangystau regions hold substantial potential for power generation using the Organic Rankine Cycle (ORC), a technology well-suited for harnessing low-enthalpy geothermal energy. The ORC can enhance energy independence and reduce reliance on fossil fuels.

In 2015–2016, prospecting and deep exploration drilling at the Zharkunak site assessed the sufficiency of geothermal resources for direct use. The project successfully leveraged geothermal wells for heating and other uses, demonstrating the feasibility of geothermal energy for sustainable development. The wells of the Zharkent basin, such as well No 5539, with temperatures exceeding 100 °C, are particularly promising for electricity generation, as they provide the steam necessary for turbine operation Figs. 3 and 4.

2.1.3. Sustainability and integration

Using existing geothermal wells for electricity production aligns with Kazakhstan's efforts to decarbonise its energy sector and integrate renewable energy sources. This study evaluates the potential of wells in the Almaty region, specifically the Zharkent depression and the Zharkunak field, as well as well No 5539, for power generation using Organic Rankine Cycle (ORC) technology. By leveraging these local geothermal resources, Kazakhstan can significantly reduce its reliance on coal-fired power plants, contributing to a more sustainable and decentralised energy system.

In addition to geothermal potential, the Zharkent region is supported by existing electrical infrastructure, including nearby substations and medium-voltage transmission lines. This fact facilitates the integration of future ORC-based geothermal power plants into the local grid, ensuring stable energy delivery without the need for substantial network upgrades [19].

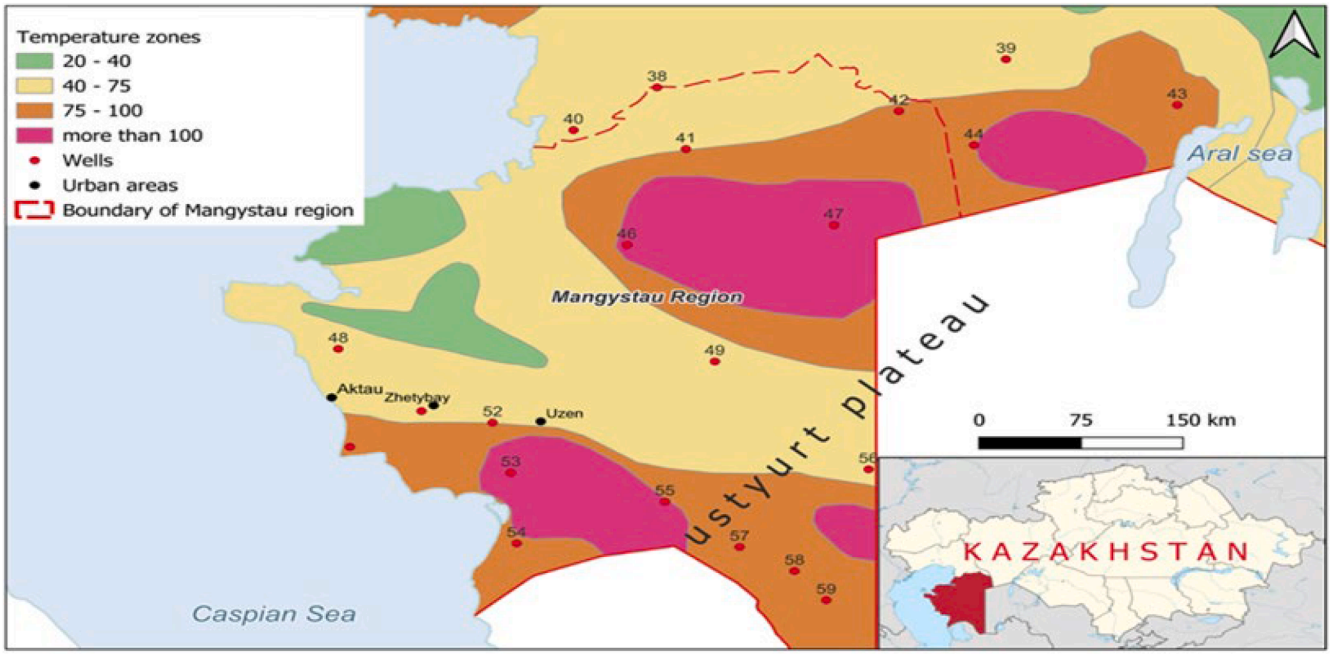

Fig. 2. Map of the occurrence of underground sources of geothermal waters in the Mangistau region. The lower-right image is the location of the Mangistau region in the country.

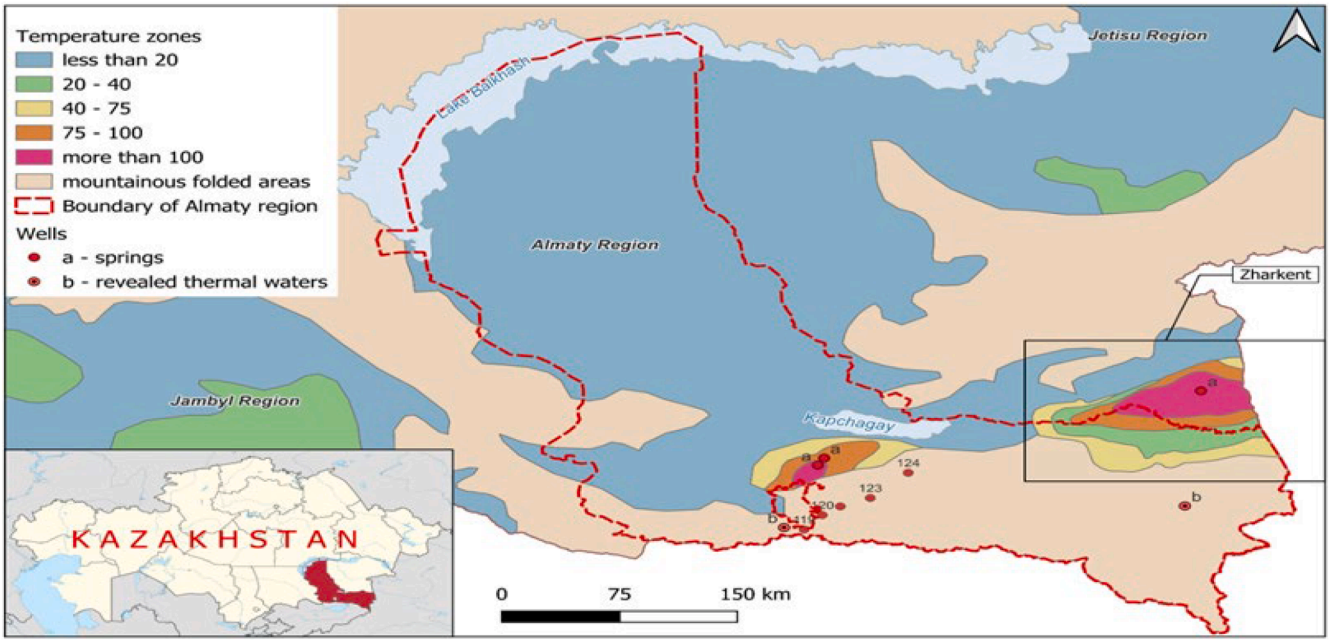

Fig. 3. Map of geothermal waters of the Almaty region. The Zharkend area, highlighted, is on the border of the Almaty region.

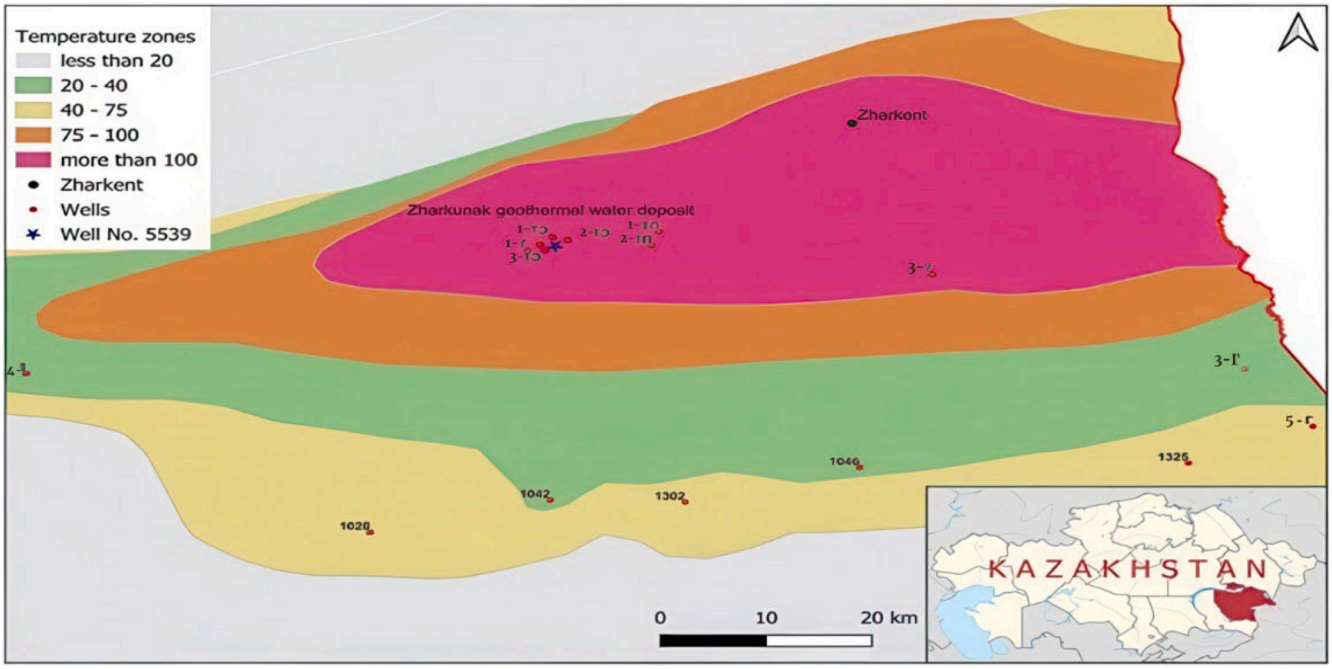

Fig. 4. This is an amplified view of Fig. 3 from the Zharkent-Almaty border.

2.2. Research method

The organic Rankine cycle (ORC) is a promising technology for small-scale power production and the exploitation of low-temperature heat sources [20]. The main difference between conventional and Organic Rankine Cycles lies in the use of an organic fluid instead of water vapour. Organic fluids, used in Rankine cycles at lower temperatures, offer practical benefits due to their favourable thermodynamic properties, such as lower boiling points compared to water. This allows the cycle to efficiently convert thermal energy into work at sources with lower temperatures, thereby improving the efficiency and viability of systems like geothermal power plants and waste heat recovery in industrial processes. Organic fluids enable these systems to operate effectively where traditional water-steam cycles would not even operate. The ORC system is more efficient, flexible, and safe than conventional energy systems. Furthermore, ORC guarantees low maintenance requirements, fast start-up and stop procedures, and efficient partial load operations [21].

In the early 1980s, Kalina proposed a new family of thermodynamically reversible heat engines for expansion and compression, utilising sources such as solar thermal, geothermal, biomass, and industrial waste heat. Moderate heat is generated from these energy cycles using a mixture of ammonia and water as the working fluid. This type of cycle configuration was called the Kalina cycle, replacing the previously used

Rankine cycle as the primary cycle for a combined-cycle power system, as well as for generating electricity using low-temperature thermal resources [22–24].

The Kalina cycle is a modified version of the Rankine cycle. The modifications that complete the cycle conversion from Rankine to Kalina consist of proprietary system designs that specifically exploit the advantages of the ammonia-water working fluid. These unique designs, used individually or in various combinations, comprise the Kalina family of distinctive cycle systems. This is analogous to the Rankine cycle, which essentially has many design variations such as reheat, regenerative heating, supercritical pressure, dual pressure, etc., all of which can be applied in various combinations [25,26].

Compared with the Rankine cycle, the Kalina cycle has similar devices in the cycle configuration. However, the Kalina cycle has one more degree of freedom than the Rankine cycle, which is the ammonia-water mixture fraction. Therefore, the thermodynamic performance of the Kalina cycle will largely depend on the ammonia-water mixture fraction and the parameters of the devices in the cycle. Regarding the ammonia-water mixture fraction, the design studies of the Kalina cycle for low-temperature and moderate-temperature geothermal resources indicate different ammonia-water mixture compositions, typically around 70 wt % ammonia [22,24,25].

Theoretically, the Kalina cycle can help convert approximately 45 % of the heat consumed by a direct-fired system into electricity and up to 52 % for a combined cycle plant (a gas turbine produces exhaust gases that enable a steam turbine to produce electricity). This compares to approximately 35 % and 44 % for a steam cycle [26,27]. Furthermore, Kalina cycles can yield up to 32 % more energy by using industrial waste heat compared to a conventional steam Rankine cycle. However, the Kalina cycle performs better than a traditional steam Rankine cycle in small direct-fired biomass cogeneration plants [27].

Additionally, the ammonia and water working fluid in a Kalina cycle plant presents material issues that differ from those in a conventional steam plant. Oxidation of plant components throughout the power cycle is less likely because oxygen levels in the working fluid are deficient. However, nitriding of high-temperature components is an issue that must be considered when selecting superheater, reheater, and high-temperature turbine components [21]. Except for turbines and superheaters, temperatures are low enough that carbon steels can be used [25]. Regarding turbine design, copper-based alloys are susceptible to corrosion in ammonia, so that some material substitution may be required [27].

Corrosion and scaling continue to be persistent challenges in geothermal energy systems, especially in heat exchangers and piping exposed to chemically aggressive fluids. Penot et al. [28] conducted a comprehensive study on geothermal installations in France, demonstrating that mild steel and aluminium alloys show poor resistance under such conditions. In contrast, high-performance stainless steels and titanium alloys provide significantly better durability. Their findings highlight that the extent and nature of corrosion are heavily influenced by the choice of working fluid—particularly in ORC systems—making fluid selection a crucial factor in determining material compatibility. This relationship is addressed in Section 3, where the evaluation of organic fluids comes before identifying suitable metallic materials for geothermal applications.

The climate affects the performance of any thermal power cycle, and therefore the exploitable resource. One of the first conditions, thus, is the evaluation of resources based on local environmental conditions. In a continental climate like Zharkent's, summers are typically hot and dry. At the same time, winters can be freezing and somewhat snowy. This results in a wide range of temperatures throughout the year. For instance, during the summer, temperatures can climb well above 30 °C, occasionally reaching 40 °C in the hottest periods. In contrast, winter temperatures can drop to −20 °C, especially during the coldest nights of December and January, in the lower regions.

These temperature variations influence the thermal efficiency of the ORC system. The first concern is to evaluate the Carnot efficiency, i.e., if the temperature range in which the machine will operate justifies the investment. The Carnot efficiency is given by Eq. (1).

$$\eta_{Carnot} = 1 - \frac{Tc}{Th} \tag{1}$$

where T_C is the absolute temperature (in Kelvin) of the cold reservoir, and T_h is the absolute temperature of the hot reservoir. As previously discussed, seasonal variations in ambient temperature significantly affect the performance of Organic Rankine Cycle (ORC) systems by altering the temperature of the cold reservoir. In the Zharkent basin, summer air temperatures can reach up to 40 °C (313.15 K), while winter temperatures commonly drop to −10 °C (263.15 K) [29]. This variation has a direct impact on the theoretical efficiency limits of the system, as described by the Carnot efficiency. The Carnot efficiency defines the maximum possible efficiency of any heat engine converting thermal energy into work, and it depends exclusively on the temperatures of the heat source and the heat sink. In this study, the hot geothermal fluid serves as the high-temperature reservoir. At the same time, the atmosphere functions as the cold reservoir, given the absence of a large nearby body of water. For modelling purposes, the average summer and winter air temperatures are adopted as reference values for the heat sink. Table 4 presents the corresponding Carnot efficiencies calculated for ORC systems operating under the thermal conditions of the Zharkent geothermal wells.

As expected, Carnot's efficiency varies significantly between summer and winter. This preliminary assessment indicates that Well 1046 is unsuitable for ORC deployment, as it yields a Carnot efficiency of <1 % under summer conditions. By contrast, Wells 48 and 3-T achieve summer efficiencies of 1.9 % and 7.5 %, respectively, increasing to 17.5 % and 22.2 % in winter, when the greater temperature differential enhances heat exchange performance.

However, real thermal efficiency is inherently lower than the Carnot limit due to unavoidable irreversibilities and engineering constraints. These include friction, turbulence, heat losses, non-isothermal heat transfer, finite-time processes, and material limitations. Additional losses arise from exergy destruction linked to entropy generation, as well as design, operational, economic, and regulatory constraints.

Based on these considerations, the most promising candidates for year-round ORC operation are Wells 5539, 1-RT, and 2-TP. Although summer performance is lower, these wells maintain sufficient thermal potential to ensure viable system operation, as summarised in Table 4.

2.2.1. *Methodological steps and the thermodynamic model*

Fig. 5 presents the methodological flowchart outlining the stages of the study. The modelling process begins with the definition of input parameters, namely the fixed thermophysical properties and flow characteristics of geothermal waters. The first modelling step comprises four parts: (1) quantifying the thermal power available in the wells (as detailed in the subsection The power available in the wells); (2) constructing a single-loop thermodynamic model based on a simplified Organic Rankine Cycle (ORC)a streamlined variation of the Kalina cycle; (3) establishing operating assumptions for system components such as turbine, heat exchanger, and generator efficiencies; and (4) computing

Table 4
Carnot's efficiency for the Organic Rankine Cycle.

Well, name or number	Temperature at the wellhead (K)	Carnot's Efficiency Summer Tc=313.15 K (%)	Carnot's Efficiency Winter Th=263.15 K (%)
1046	315.6	0.8	16.6
48	319.2	1.9	17.5
3-T	338.5	7.5	22.2
5539	376.2	16.7	30.0
1-RT	371.2	15.6	29.1
2-TP	360.4	13.1	27.0

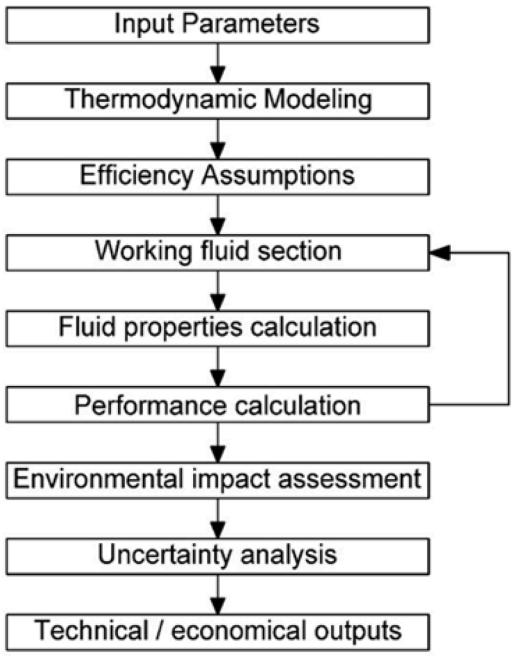

Fig. 5. Methodological flowchart for evaluating a geothermal ORC system.

fluid properties across each stage of the cycle to determine net work output. This stage uses R-407 as the reference organic fluid, with results presented in the "Power of the Cycle" subsection. The model is applied to estimate electricity production in the Almaty region, thereby concluding the performance assessment phase and Section 2.

Section 3 presents a sensitivity analysis evaluating alternative working fluids, supported by an iterative loop (Fig. 5), which enables performance evaluation through fluid selection. An environmental impact assessment follows, which includes an evaluation of organic fluid emissions and potential carbon savings resulting from geothermal deployment. The methodology is completed with uncertainty analysis and a techno-economic assessment, providing insight into model robustness and project feasibility.

The selected model is deliberately simplified to estimate electricity production potential rather than optimise detailed ORC design. It comprises four core components: evaporator, turbine, condenser, and pump. This abstraction facilitates an initial assessment of the viability of multiple geothermal ORC systems across the Zharkent basin. The geothermal water enters the evaporator, serving as the primary heat source. The model adheres to a control volume approach consistent with the formulation in [30], with governing equations accessible in standard thermodynamics references such as [31] and [32]. A schematic of the ORC configuration is provided in Fig. 6(a).

In this case, the selected model will evaluate the electricity production potential rather than assess the ORC system's design and efficiency. One selected the simplest model, consisting of an evaporator, turbine, condenser, and pump, to evaluate the possibility of multiple geothermal ORC systems in the Zharkent basin. The geothermal hot water will be directed into the evaporator, acting as the primary heat source. The model was designed based on the control volume concept discussed in [30]. The derived equations can be found in any standard engineering thermodynamics reference, such as [31] or [32]. The model is depicted in Fig. 6(a).

2.2.2. *The power available in the wells*

Due to the absence of operational geothermal power plants using ORC technology in Kazakhstan, direct calibration of the model using local experimental or field data was not feasible. Accordingly, the model was not calibrated with site-specific datasets. Instead, its reliability was assessed through comparative validation using performance parameters published in the international literature for real-world ORC systems operating with low-enthalpy geothermal resources. Reference studies include Astolfi et al. [33], which examined binary ORC units optimised for heat sources up to 120 °C, and Yu et al. [34], which presented thermodynamic evaluations of ORC systems using direct evaporative condensers. These sources provide typical operational ranges for thermal efficiency and power output, offering a relevant empirical basis for verifying the coherence of the simulation outputs generated in this study.

To access the power in the well, one must present two hypotheses: the well pressure and the type of soil. Since the well pressure is unknown, a conservative value of 3000 kPa was assumed. It is unlikely that self-draining geothermal wells will have lower static pressures. The second hypothesis is that the existing soil type affects the heat transfer efficiency from the well to the evaporator. Thus, the ORC's efficiency is directly influenced by the geological structure of the land of the Zharkent source. Given that the land in the Zharkent source is sandy in these wells, it could boost the well-evaporator heat transfer efficiency by up to 40 % [35].

It was assumed that the heat transfer efficiency between the geothermal well and the evaporator is 40 %. This value represents the typical thermal losses observed in sandy and unconsolidated sedimentary formations when there is no active well insulation. Similar efficiency levels have been reported in medium-depth geothermal systems operating in aquifers with high porosity and thermal conductivity [36, 37]. This assumption is considered applicable to the southern regions of Kazakhstan, including the Zharkent area, where comparable geological

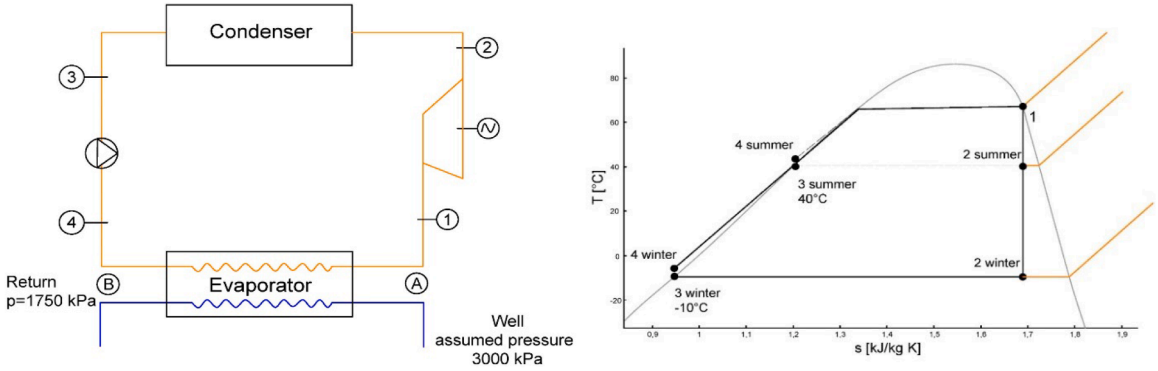

(a) (b)

Fig. 6. (a) Typical layout of water line in blue. Water circulation from A to B; ORC fluid in orange; ORC circulation from 1 to 2–3–4; **(b)** the R407c temperature and entropy evolution as it moves in the different parts of the circuit: 1–2 expansion turbine; 2–3 condenser; 3–4 pump; 4–1 evaporator.

conditions prevail. The influence of this parameter is further assessed through a sensitivity analysis, as it is one of the key factors in the model. The realism of the assumed efficiency is supported by transient heat transfer modelling in geothermal wells [36] and by thermal performance evaluations of medium-depth geothermal systems [37].

The well heat capacity is calculated by considering the heat balance between points A and B, representing the well tap's inlet and outlet, Fig. 6(a). This method allows us to determine the heat power of the well accurately, given by:

$$\dot{Q}_{well} = \dot{m}(h_B - h_A) \tag{2}$$

where h_B- may present a lower return pressure due to the head loss. The mass flow is calculated from the volumetric flow, or the debit, by the fluid's density:

$$\dot{m} = \rho \cdot \dot{v} \tag{3}$$

The evaluation of each well's available heat power was made after the determination of the thermodynamic properties of the water's vapour. The se properties were obtained from CoolProp [38] software and are depicted in Table 5. CoolProp is an open-source library that provides reference-quality thermodynamic properties for several fluids, including water. The fluid's properties were obtained to support the previously discussed hypotheses, assuming an atmospheric baseline condition: the average summer temperature was 40 °C and −10 °C for winter; the pump inlet pressure was 3000 kPa to ensure that the outlet pressure was a minimum of 1750 kPa. The pressure in geothermal wells that self-drain can vary depending on the design, location, and operational conditions. Generally, pressure is regulated to optimise energy extraction and maintain the well's stability. Pressure in wells can range from low values close to atmospheric pressure, such as those in open systems, to much higher pressures in deeper or more confined systems. The estimation of water pressure was based on the hypothesis of a minimum of 3000 kPa since no pressure measurements were available. By underestimating the well's pressure, one ensures that the well's heat power assessment results are conservative.

Eq. (2) gives the heat power. The heat power capacity is provided by the enthalpy gradient of the well inlet and outlet, multiplied by the geothermal water mass flow [32]. The mass flow was calculated by multiplying the volumetric flow rate by the water density at the specific temperature and pressure conditions, as shown in Eq. (3).

The geothermal hot water is the primary heat source and is directed into the evaporator. Inside the evaporator, the geothermal hot water flows through a series of pipes or coils, part of a closed loop containing an organic working fluid. The heat carried by the geothermal vapour will be transferred to the circuit's organic working fluid. The quantity of heat transferred to the organic fluid can be estimated as indicated in Eq. (4), where $\dot{Q}_{well}$ is the heat power of the well and η_{well} is the efficiency of the heat transfer from the well to the evaporator, $\dot{Q}_{evap}$. One assumed a 40 % efficiency in heat transfer, supported in the literature [32].

$$\dot{Q}_{evap} = \eta_{well} \cdot \dot{Q}_{well} \tag{4}$$

Eq. (5) provides the heat available from the well, where the well's flow rate, the water's specific heat, and the outside environment's temperature are considered in any given season.

$$\dot{Q}_{well} = \dot{m} \cdot c_p (T_A - T_e) \tag{5}$$

Table 6 summarises the assumed efficiency values for the key components of the ORC system. The turbine efficiency was set at 0.80, consistent with recent studies reporting isentropic efficiencies of approximately 80 % for radial-inflow turbines in small-scale ORC applications [39]. The generator efficiency was assumed to be 0.70, reflecting typical conversion losses observed in decentralised ORC systems when transforming mechanical to electrical energy [40]. The heat exchanger effectiveness was estimated at 0.40, a representative value for geothermal ORC systems operating under subcritical conditions with moderate temperature gradients [41].

The parameters used in Eqs. (4) and (5) to calculate the available thermal power are listed in Table 7. Table 8 presents the resulting thermal power values under both summer and winter conditions, derived using Eq. (2) and the temperature and mass flow properties for stations A and B provided in Table 5. As shown, Well 5539 exhibits the highest available thermal power in both seasonal scenarios, delivering nearly 8.4 MW of heat to the circuit, which makes it the most promising candidate for electricity generation among the wells analysed.

2.2.3. The power of the cycle

Table 8 presents the estimated seasonal thermal capacity of each well, indicating the maximum exploitable energy and reflecting variations in resource availability and suitability for electricity generation. However, the electric power extracted from the geothermal well will be a fraction of that, as clearly defined by the Second Law of Thermodynamics. With this limitation in mind, a simple thermodynamic model can be applied to evaluate the extractable resource of each well, as depicted in Fig. 6.

As the geothermal hot water circulates in the evaporator, it transfers heat to the organic working fluid, causing it to evaporate and generate high-pressure vapour—process 4–1 in Fig. 6. The selected organic fluid is R407c, chosen for its thermodynamic properties [42,43], including a low boiling point and high vapour pressure, which are ideal for these low-temperature wells. R407c was chosen once its critical temperature was 10 K above the maximum well temperature. The phase change of R407c occurs efficiently in the evaporator, minimising thermal losses through a suitably designed large surface [44,45].

The criterion for selecting the organic fluid was determined by the temperature of point 1 of the organic fluids cycle. When the fluid is at Quality equal to 1 and a pressure of 3000 kPa, its temperature must be lower than the well's 2-TP temperature, i.e. 87.2 °C. If the fluid's evaporation is higher than the wells' temperature, it cannot be used to absorb the geothermal heat. For this part of the circuit analysis, one will reference the R407c organic fluid. The influence of different organic fluids will be explored further in the subsection on Fluid selection criteria.

The high-pressure R407c vapour leaves the evaporator and goes into a turbine. The turbine expands and spins the blades, converting thermal

Table 5
Geothermal water properties in the evaporator's inlet and outlet.

					Entrance point – Point A		
	Wells	T (°C)	T (K)	ρ (kg/m^3)	h (kJ/kg)	s (kJ/kgK)	$\dot{m}=\rho x \dot{v}'$ (kg/s)
Point A - p = 3000 kPa	5539	103.0	376.2	956.145	437.047	1.342	48.25
	1-RT	98.0	371.2	959.754	410.966	1.285	23.23
	2-TP	87.2	360.4	967.151	365.521	1.161	28.14
Point B - p = 1750 kPa		40.0	313.2	992.210	167.615	0.572	
Point B - p = 1750 kPa		0.0	273.2	999.700	0.42117	0.151	

Table 6
Assumed equipment performance efficiencies.

Constant	Value
turbine efficiency	0.80
electric generator	0.70
heat exchanger	0.40

Table 7
Geothermal water properties of the three chosen wells.

Wells	$\dot{m}$ (kg/s)	c_p (kJ/kg K)	T_A (°C)	T_B Winter (°C)	T_B Summer (°C)
5539	48.25	4.2192	103.0	−10.0	40.0
1-TR	23.23	4.2134	98.0	−10.0	40.0
2-TP	28.14	4.2026	87.2	−10.0	40.0

Table 8
The available thermal capacity of the wells under study.

Wells	Available heat power – Summer (MW)	Available heat power – Winter (MW)
5539	5.130	8.305
1-TR	2.270	3.797
2-TP	2.232	4.077

into mechanical energy—Process 1–2 in Fig. 6. A shaft connects the turbine to an alternator that converts the mechanical energy into electrical energy. The fluid's pressure and temperature drop after the turbine, but it maintains a saturated state, where vapour and liquid coexist. For summer conditions, the fluid's quality will be 97.8 %, i.e., the R407c will be vapour. In winter, pressure and temperature drops will be higher, thus condensing more fluid. After the turbine, 95.8 % of the circulating R407c will be vapour. A 4.2 % condensate is within the acceptable operation limits of a vapour turbine [32,46].

After passing through the turbine, the R407c vapour is condensed back into a liquid by a cooling system—process 2–3. In our case, this is an air-cooled condenser. A pump then circulates the liquid back into the evaporator to repeat the cycle, process 3–4.

For all processes, a steady state condition has been assumed for two seasons for a system operating with R407c. System components' pressure drops and heat losses should be addressed [44–47]. Fig. 6(b) shows the T-s diagram of this process, and the fluid's properties are depicted in Table 9. The table shows the properties of the organic liquid R407c obtained from [31] and the schematics of the T-s R407c depicted in Fig. 6(a).

A control volume at the evaporator allows for calculating the R407c mass flow rate, as Eq. (6) depicts. The heat $\dot{Q}$ is provided in Table 10, and the enthalpy is in Table 5.

$$\dot{m} = \dot{Q}/(h_1 - h_4) \tag{6}$$

The required mass flow rates of R407c for different seasons is 31.517 kg/s in summer for well 5539 and 32.872 kg/s in winter. Also, for wells 1-RT and 2-TP in summer, 13.950 and 15.030 kg/s, and in winter, 13.717 and 16.138 kg/s. Table 10 presents the mass flow of R407c for both seasons.

The mass flow rates of the working fluid R407c were calculated using the energy balance at the evaporator (Eq. (6)), with enthalpy values drawn from Table 9. This approach ensures consistency between the available thermal energy and the required heat input under the defined seasonal operating conditions.

The vapour turbine's maximum power is also determined by applying a control volume [30]. The fluid's enthalpy is presented in Table 9. For simplicity, one assumed the turbine's efficiency to be 80 %. Note that this value was used to calculate the mechanical power, not the properties of point 2 of the assumed isentropic expansion.

Table 9
Thermodynamic properties of R407c for the summer and winter conditions.

Point	P (kPa)	T (K)	v (m^3/kg)	h (kJ/kg)	s (kJ/kgK)	x (%)
1	3000	363.15	0.00575	436.130	1.6995	–
2 summer	1750	319.46	0.01645	419.076	1.6995	97.83
2 winter	404	262.92	0.20826	366.010	1.6995	95.84
3 summer	1750	313.15	0.00087	256.540	1.1909	–
3 winter	404	263.15	0.00076	186.720	0.9507	–
4 summer	3000	313.15	0.00087	256.540	1.1909	–
4winter	3000	263.65	0.00076	186.720	0.9507	–

Table 10
The R407c required mass flow $\dot{m}_s$ for summer and $\dot{m}_w$ for winter.

Wells	$\dot{m}_s$ (kg/s)	$\dot{m}_w$(kg/s)
5539	31.517	32.872
1-TR	13.950	15.030
2-TP	13.717	16.138

$$\dot{W}_{turb} = \dot{m}(h_1 - h_2)\cdot\eta_{tur} \tag{7}$$

where: η_{turb}=0.80

The system's net power is given by the difference between the work obtained in the turbine expansion and pumps, calculated as indicated in Eq. (8), [30].

$$\dot{W}_{pump} = \dot{m}\ v\ \Delta P \tag{8}$$

where v is the specific volume of the flow. As expected, the work from the pumps can be ignored once calculations show it to be 0.01 % of the turbines' total expansion work.

The overall energy that can be extracted from each well is thus presented in Table 11. Well 5539 has the highest available thermal capacity, with an electricity production potential of 825.0 GWh in summer and 4 507.1 GWh in winter. As expected, the values are significantly higher in winter than in summer because heat exchange will be much more efficient in winter due to larger temperature differences. For wells 1-TR and 2-TP, the available electricity production in summer is 363.3 and 357.2 GWh, and in winter, 2 057.7 and 2 209.8 GWh, Table 11.

Electrical output values were obtained from thermodynamic ORC simulations using R407c, incorporating seasonal temperature variations based on regional climatic data. These outputs formed the basis of the thermodynamic model, enabling evaluation of the ORC system's efficiency under different operating conditions. However, the developed model is based on steady-state conditions and does not account for the dynamic behaviour of the geothermal reservoir, including temporal variations in pressure and temperature (e.g., thermal depletion or reservoir pressure decline). Hydraulic losses in pipelines and heat exchangers are not considered, and the system is assumed to operate under nominal full-load conditions. The part-load operation, which may occur due to seasonal or fluctuating demand, is also not included at this stage. These simplifications are justified by the conceptual nature of the study and are intended to enable a preliminary evaluation of the ORC system output. Future research will address these effects using more advanced modelling tools that can more accurately reflect real-world operating conditions. For example, recent studies on the Yangyi geothermal field [37] have simulated pressure and temperature variations as well as two-phase flow in the wellbore, providing valuable insights for further refinement of our model.

The efficiency of the geothermal system was calculated based on the data in Tables 8 and 11, which present the input (thermal) and output (electrical) energy values for the studied wells. For well No 5539, the calculated cycle efficiency was 11.86 %, which is naturally lower than the theoretical Carnot efficiency (16.7 % in summer and 30.0 % in winter). This value accounts for thermal losses and the characteristics of

Table 11
Possible extracted geothermal energy for the model operating with R407c organic fluid.

Wells	Summer (GWh)	Winter (GWh)
5539	825.0	4 507.1
1-TR	363.3	2 057.7
2-TP	357.2	2 209.8

low-temperature sources, confirming the realism of the model. Moreover, the obtained results are consistent with those of Astolfi et al. [33], who demonstrated that binary ORC systems operating with heat sources up to 120 °C achieved thermal efficiencies ranging from 8 % to 12 %, depending on the cycle configuration and working fluid. Thus, the model exhibits performance values typical of real-world installations and is applicable for assessing the potential of ORC technologies in this region of Kazakhstan.

3. Results

3.1. Estimated electricity production in the Almaty region

The final part of the model estimates electrical production from the three geothermal wells, as shown in the Table 11. The potential electricity production, *E*, is calculated from the energy generated by the turbines in summer and winter by each machine's full power operating time, *t*, by the electrical efficiency, Eq. (9).

$$E = P \cdot t \cdot \eta_{electric} \quad (9)$$

In this model, the electrical efficiency is 98 %, and turbines operate at 90 % of their nominal capacity 90 % of the time, with 10 % allocated for downtime operations or maintenance. Therefore, the available geothermal energy depicted in Table 11 can be converted into electricity, as shown in Table 12. Eighty-five per cent of the electricity production will occur during the winter, which is related to the overall system efficiency, as indicated by the thermodynamic system and local weather conditions.

Tables 11 and 12 present the seasonal and annual geothermal energy production for each well using R407c. The results highlight the system's sensitivity to reservoir temperature, with notable differences in performance between summer and winter. R407c demonstrates relatively stable output across both conditions; however, the choice of working fluid remains a critical factor influencing thermal efficiency and total energy yield. These findings emphasise the importance of fluid selection and temperature conditions in optimising ORC system performance.

3.2. Sensitivity to different organic fluids

The electricity production estimate in Table 12 was calculated for R407c organic fluid. However, selecting an organic working fluid depends on several criteria, including the nature of the heat source, turbine and pump costs, and the properties of the fluid. Key variables in fluid selection include the saturation vapour curve, low freezing point, high stability temperature, high heat of vaporisation and density, viscosity, heat transfer characteristics, low environmental impact, safety, good availability, low cost, acceptable pressures, and compatibility of materials. Choosing the proper working fluid is crucial for the cycle's operation and efficiency.

The selection of working fluid has been discussed in many scientific articles and specific engineering reports [48–50]. Many articles primarily address the thermo-physical properties of working fluids, emphasising cycle efficiency, thermal efficiency, network output, second law efficiency, and so on. The types of working fluids include dry, wet, and isentropic fluids. A dry fluid has a positive slope on the saturation curve of a T-s diagram; a wet fluid has a negative slope; and an isentropic fluid features an infinitely large slope. Generally, dry and isentropic fluids are more effective for power plants based on the organic Rankine cycle.

This study was further developed by extending the potential geothermal power output through the examination and calculation of 14 fluids for three wells across both seasons. This yielded 84 possible values for electricity production, of which 78 are feasible. The properties of the three wells were calculated for the winter and summer seasons.

The power output depends on the physical state, pressure, and temperature of the working fluid. Three tools were used to find these properties: the Coolpack software [51] from the Technical University of Denmark (DTU), the Pyromat property Calculator [52], a Python thermodynamics property library, and Thermostate [53], a property calculator software. All three were used to check the properties of the working fluids.

The model's parameters and electricity production were recalculated for an additional 14 organic fluids as exemplified in Tables 9–12. One will refrain from presenting the respective 52 intermediate tables for the three wells. Table 13 summarises the estimated electrical production for all these fluids. The fluid selection considered the fluid's critical point, phase change properties, and the high-pressure circuit line of 3000 kPa. Eleven fluids were identified that fulfil the operating conditions requirements of all three wells. Two fluids are unsuitable for well 1-TR: R-1234ze(E) and R-227ea; and three are unsuitable for well 2-TP: R12, R-1234ze(E) and R-227ea.

Fig. 7 presents a bar chart comparing the estimated annual electricity generation for each of the working fluids analysed in this study. These results reflect the thermodynamic properties of the fluids and support the selection of R-152a as the most efficient and environmentally friendly working fluid. The visual representation complements the numerical data provided in Table 13 and clearly illustrates the differences in performance among the tested fluids.

The results vary for all three wells, with improved electrical production achieved by switching from R407c to another organic fluid (Fig. 8). If R12 is used, the electricity production of well 5539 will increase by 31 %. Better performance is also achieved by adopting R-227ea, R-1234ze, or R-134a. The productivity improvement of 4 % for well 1-TR is less remarkable when replacing the fluid with R12 or R154a compared to well 5539. By replacing R407c with R152a, the production improvement in well 2-TP will be only 2 %.

Figs. 7 and 8 further illustrate the significant impact of working fluid selection on the efficiency of an ORC system. Wells with higher

Table 12
Model's estimated geothermal electricity production (GWh) for the model operating with R407c organic fluid.

Wells	Summer	Winter	Yearly Production (GWh)	Geothermal Production Break-down (%)
5539	825.0	4 507.1	5 332.1	51.66
1-TR	363.3	2 057.7	2 421.1	23.45
2-TP	357.2	2 209.8	2 567.1	24.89
SUM			10 320.3	100.00

Table 13
Total annual production results for each well. The results reflect the simulated performance of the ORC system across a range of working fluids.

Organic Fluids	Total Electrical Production [GWh]		
	Wells		
	5539	1-TR	2-TP
R12	6 981.2	2 506.9	–
R-1234ze(E)	5 485.6	–	–
R134a	5 056.3	2 287.4	2 405.9
R-152a	5 467.0	2 471.3	2 597.9
R-161	4 759.6	2 151.8	2 268.5
R-227ea	5 724.9	–	–
R143a	3 905.4	1 769.2	1 870.6
n-propane	4 478.1	1 842.3	1 958.5
R115	4 455.6	2 016.6	2 122.5
R22	4 518.0	2 046.9	2 160.3
R404a	3 872.1	1 754.6	1 854.9
R407c	5 332.1	2 421.1	2 567.1
R507a	3 808.7	1 726.1	1 825.5
R125	3 610.2	1 637.3	1 733.2

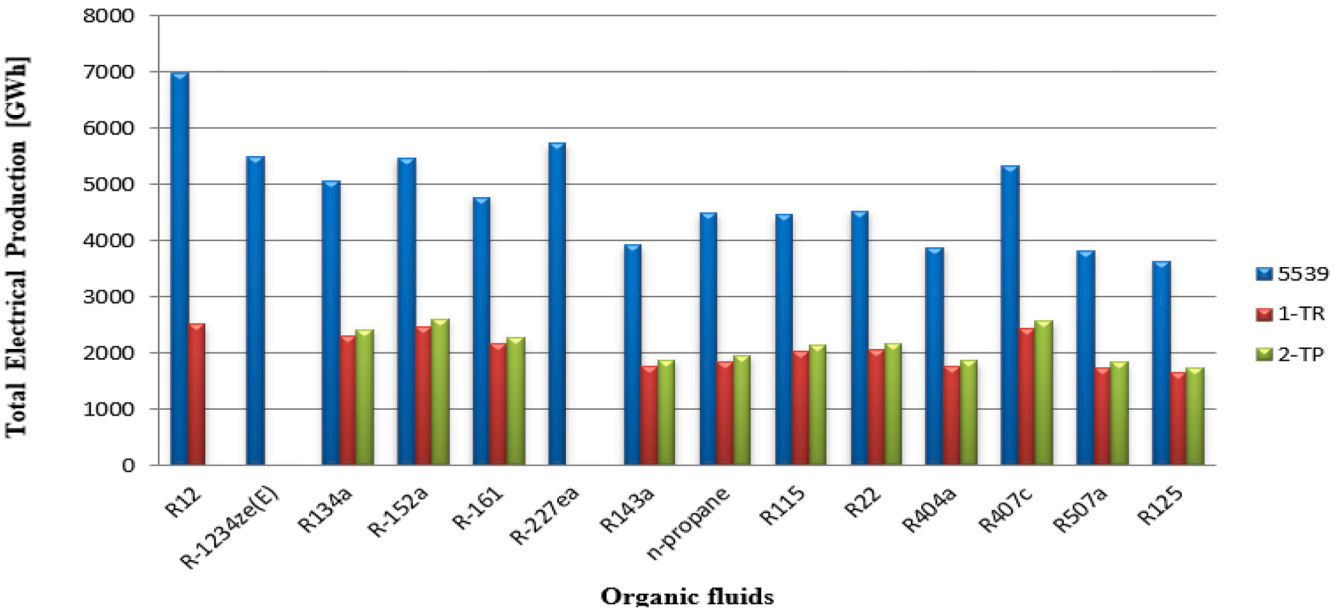

Fig. 7. Performance comparison of selected working fluids based on annual electricity production.

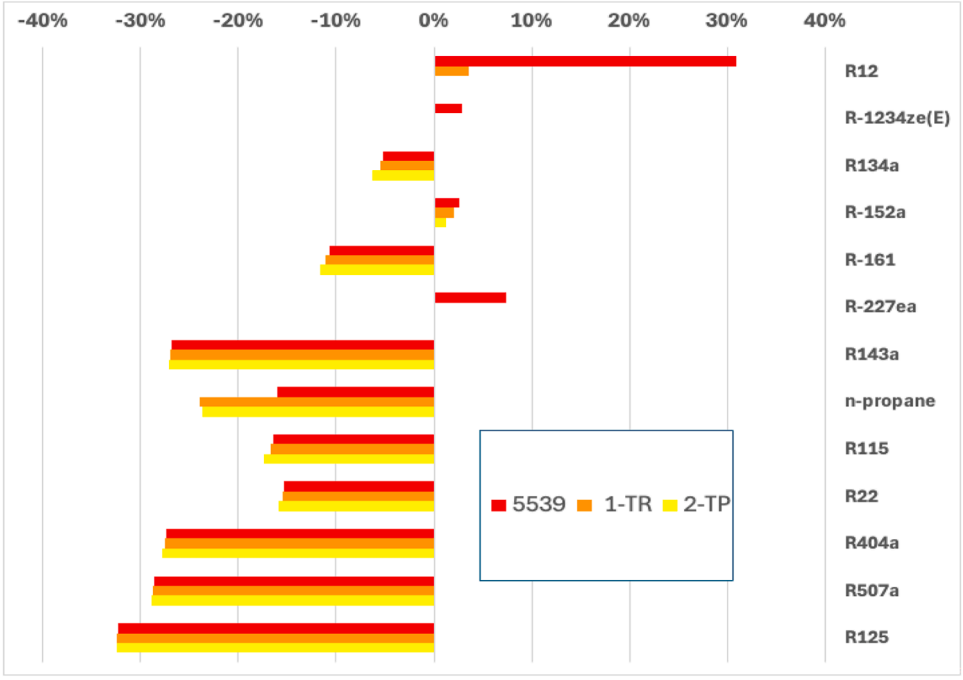

Fig. 8. The model's relative power output increases and decreases by changing the organic fluid from R407c (based on the absolute values of (Table 13).

temperature and enthalpy, such as Well 5539, exhibit greater sensitivity to fluid substitution, underscoring the strong coupling between reservoir conditions and the thermophysical properties of the working fluid. These findings reinforce the importance of site-specific optimisation in geothermal system design.

The increase in productivity is not the only variable to consider. Environmental factors such as Ozone Depletion Potential (ODP) and Global Warming Potential (GWP-100-year), along with operational aspects like flammability and toxicity, must also be included in the evaluation. Table 14 summarises the key figures for these fluids.

The values of Ozone Depletion Potential (ODP) and Global Warming Potential (GWP, 100-year horizon) are taken from the Kigali Amendment to the Montreal Protocol [54] and ASHRAE Standard 34 [55]. Flammability classifications follow ASHRAE guidelines [55] and experimental results reported by Kondo et al. [56].

The first fluid analysed was dichlorodifluoromethane (R-12), a colourless gas commonly known by the trade name Freon (Freon-12). R-12 belongs to the group of chlorofluorocarbons (CFCS). The stability of CFCS, coupled with their chlorine content, has linked them to the depletion of the Earth's protective ozone layer. This gas has been globally banned since 2010 under the Montreal Protocol, signed in 1988. Kazakhstan adheres to this ban. It serves as the baseline for the ozone depletion potential (ODP), which is 1.0. Its global warming potential (GWP) over 100 years is 10,900, meaning that over 100 years, 1 kg of R12 will trap 10,900 times more heat than 1 kg of CO_2. The following possible fluids are our reference fluid R407c, a ternary

Table 14
Properties of liquids by Ozone depletion potential and global warming.

Refrigerant	ODP	GWP (100-yr)	Flammability
R12	1.0	10,900	Non-flammable
R-1234ze(E)	0.0	6	Mildly flammable
R134a	0.0	1430	Non-flammable
R-152a	0.0	124	Mildly flammable
R-161	0.0	4	Mildly flammable
R-227ea	0.0	3220	Non-flammable
R143a	0.0	4470	Non-flammable
n-propane	0.0	3	Highly flammable
R115	0.6	7370	Non-flammable
R22	0.05	1810	Non-flammable
R404a	0.0	3922	Non-flammable
R407c	0.0	1774	Non-flammable
R507a	0.0	3985	Non-flammable
R125	0.0	3500	Non-flammable

zeotropic HFC mixture composed of R32, R125, and R134a in a mass ratio of 23:25:52. R407c's ozone depletion potential (ODP) is zero, while its Global Warming Potential (GWP-100-yr) is 1774. R1234ze(E) is a medium-pressure refrigerant classified as a flammable refrigerant (A2L) according to the ASHRAE 34 standard [55]. It has no ozone depletion potential (ODP), and its global warming potential (GWP) over 100 years is 6 (Table 14). Despite its low flammability, R1234ze(E) can reduce the flammability potential of other liquids. For instance, when mixed with ammonia, the combustion capacity of a pure refrigerant may decrease [56]. Furthermore, R1234ze(E) possesses both advantages and disadvantages that prevent it from serving as an alternative to low Global Warming Potential (GWP-100-year) refrigerants currently in use, such as R134a, R404A, R410A, and R22. Due to its similar normal boiling point ($T \approx 256$ K), the refrigerant R-227ea can be used as an alternative to R-12 and R-114. It is suitable for installations with high condensation temperatures, such as high-temperature heat pumps. In addition to refrigeration units, it is also beneficial for firefighting and fuel applications. It has no ozone depletion potential (ODP), and the global warming potential (GWP-100-yr) is equal to 3220 (Table 14).

R-152a is a pure refrigerant made entirely of 1,1-difluoroethane ($C_2H_4F_2$) and falls into the single-component category. Its ozone depletion potential (ODP) is zero, and its Global Warming Potential (GWP-100-year) is 124.

It is used to replace R-134a in new systems. It has excellent thermal and chemical stability, low toxicity, moderate flammability, and is highly compatible with most materials. We selected R-152a as the working fluid for our ORC geothermal power plant due to its thermodynamic performance and low Global Warming Potential (GWP 124), but primarily because it remains free from the increasing environmental restrictions that threaten alternative fluids.

R-227ea and R-407c have very high global warming potential (GWP) and are subject to phase-down regulations under the Kigali Amendment [54]. Meanwhile, R-1234ze(E), despite its low GWP, is facing increasing scrutiny for being a PFAS substance and may soon encounter bans in various jurisdictions. In contrast, R-152a offers a future-proof, efficient, and regulatory-compliant solution, making it the most sustainable and responsible choice for long-term geothermal power generation.

Among all the evaluated working fluids, R-152a demonstrated the most favourable combination of high thermal efficiency and low global warming potential (GWP). Due to its environmental advantages, technical suitability, and reliable performance under local geothermal conditions, R-152a is recommended as the optimal working fluid for ORC systems in Kazakhstan.

Given this recommendation, particular attention must be paid to the operational implications of using R-152a, which is classified as mildly flammable (ASHRAE safety group A2). In this context, material selection and safety protocols become critical. The most suitable materials for heat exchangers and pipelines are stainless steels, such as AISI 316 L, and aluminium alloys, owing to their corrosion resistance, thermal stability, and compatibility with fluorocarbon-based fluids [57]. Compared to mild carbon steel, which was used in early Kalina cycle systems, these materials offer significantly improved protection against pitting and intergranular corrosion in closed-loop ORC circuits. Moreover, safety measures, including leak detection systems, automatic shut-off valves, and passive fire barriers, should be implemented by international safety standards and best practices [58,59].

4. Critical analysis

4.1. Discussion and comparison with international studies

Well, 5539 (Table 13) stands out with an annual productivity of 5 467.0 GWh of electricity, significantly surpassing that of the other wells. This result can be attributed to its notably higher temperature, as indicated in the Table 6. The total annual electric energy of wells 1-TR and 2-TP reach respectively 2 471.3 and 2 597.9 GWh. The total electric energy potential of all the wells under study is 10 536.2 GWh, underscoring the substantial potential for producing eco-friendly electricity in the Almaty region, particularly in Zharkent. This potential could be crucial in addressing the city's growing electricity deficit, offering a promising solution for a more sustainable energy future.

This study focused on two regions with almost identical energy characteristics. However, it was found that Zharkent stands out in the Almaty region due to its high energy dependency and exceptional geothermal potential. The ratio between electricity production and consumption is 12 825 GWh (output of 14 046 GWh, consumption of 26 871 GWh) [60]. The geothermal water temperature in the Zharkunak field, in the Zharkent reservoir, is the highest recorded temperature in Kazakhstan, making it a prime location for geothermal energy exploration.

Almaty's overall electricity deficit reaches 12 825 GWh, which is necessary for the grid to supply the region from other areas. Highly polluting coal thermal power plants compensate for this deficit. Local exploitation of known geothermal fields in the Zharkent reservoir could yield 10 536.2 GWh, accounting for 82.1 % of the current deficit. A commonly accepted average emissions factor for coal-fired electricity generation is 1 tonne CO_2 per MWh (Intergovernmental Panel on Climate Change (IPCC, 2006 Guidelines for National Greenhouse Gas Inventories). By adopting this type of ORC geothermal solution, 10.54 million tonnes of CO_2 will be prevented from being emitted into the atmosphere each year.

To evaluate the practical feasibility and global comparability of the proposed binary Organic Rankine Cycle (ORC) configuration, we conducted a comprehensive analysis of implemented projects and recent scientific advancements in medium-temperature geothermal applications.

In Turkey, several binary ORC plants operate in geothermal regions such as Germencik, Gümüşköy, and Kızıldere, where fluid temperatures range from 100 °C to 150 °C and net electrical outputs span 3 to 15 MW. These facilities commonly employ dual-loop configurations using fluids like R245fa, R134a, and R-1233zd(E). Although both R-1233zd(E) and R-1234ze(E) are hydrofluoroolefins, only R-1233zd(E)—a non-flammable, low-pressure HFO—is widely used in Turkish geothermal systems. In our study, we did not simulate R-1233zd(E) but tested R-1234ze(E), a chemically related but more volatile fluid, which underperformed compared to our reference, R-152a. Nevertheless, these plants demonstrate stable operation and high efficiency under medium-enthalpy conditions similar to those in Kazakhstan's Zharkent region [61–63].

In Iceland, low-temperature ORC units also show effective performance. For instance, the Flúðir system operates at around 85 °C, delivering electricity to remote communities. Despite modest source temperatures, efficiency is maintained through optimised cycle design and careful fluid selection [62].

Recent studies provide additional support for our configuration.

Komarov and Shipkov (2022) showed that multistage ORC systems using 120 °C geothermal sources could improve thermal efficiency by up to 36.5 % over baseline designs [62]—a result particularly relevant to Zharkent's 103 °C resource, suggesting ample scope for optimisation.

The projected performance of our ORC model, designed for 103 °C geothermal input, is consistent with outputs from comparable systems in Turkey and Iceland. Additionally, Zharkent's geological profile—characterised by moderate geothermal gradients and accessible aquifers—closely resembles conditions in Western Anatolia and Southern Iceland. This similarity enhances the transferability of international design principles, fluid strategies, and operational protocols to the Kazakh context.

With an estimated annual electricity production of approximately 10.5 TWh, our ORC model falls squarely within the performance range of proven international systems. This reinforces the technical viability and environmental justification for deploying binary ORC technology in geothermally active regions of Kazakhstan, particularly where decentralised solutions are needed to address electricity deficits.

4.2. Technical-economic uncertainties

The results will be incomplete without an uncertainty analysis of the geothermal resource. When assessing the geothermal resource, it is essential to remember that subsurface conditions significantly contribute to the uncertainty in geothermal ORC forecasts [63,64]. A Monte Carlo sensitivity study on geothermal ORC power output highlights that reservoir temperature is the most influential factor, significantly affecting power estimates [64]. Flow rate and recovery factor, closely tied to reservoir size, notably contribute to uncertainty, while parameters such as rock heat capacity and plant uptime have a minimal impact [65]. Additionally, the decline of the reservoir, as well as mineral scaling and corrosion, can hinder operations and result in unexpected output losses [28].

Forecasting geothermal power output involves significant uncertainties, often expressed as confidence intervals or P90/P50 metrics [65]. Quantifying uncertainty is crucial for planning geothermal ORC projects. Developers present a range of outcomes (P90/P50/P10) to investors, identifying key risks such as reservoir temperature and flow capacity. By leveraging probabilistic tools, forecasters can provide realistic production estimates, enabling decision-makers to formulate effective mitigation strategies [63,66].

A U.S. DOE/NREL analysis found that for a site with an expected reservoir temperature of 120 °C, the 95 % confidence interval could range from approximately 100 °C to 140 °C [65]. Such variations can significantly impact ORC efficiency—an ORC plant at 80 °C might have an efficiency of under 10 %, while at 120 °C, it could exceed 12–15 % [66]. These values are consistent with those presented for our case as discussed in the previous subsection.

Uncertainties compound through modelling, leading to P95 estimates being 20–30 % lower than median expectations [64,65]. A renewable energy risk study found that the P90 estimate can be about 15 % below P50 [67]. In one example, a Canadian ORC project had only a 13–20 % chance of meeting an 18.9 GW/year target at a depth of 5 km, improving to approximately 38–41 % at a depth of 6 km [68]. This broadband uncertainty highlights the broad error bars in geothermal forecasts, necessitating both P50 and conservative P90 scenarios for advancing with project exploration.

Forecasts of geothermal power output are typically presented with confidence intervals to account for uncertainties related to resource availability and operational conditions. For instance, a statement such as "Project X will produce 40 GWh/year (P50), with a P90 of 36 GWh and a P10 of 44 GWh" reflects $a \pm 10$ % spread around the median and is derived from probabilistic assessments such as Monte Carlo simulations. Several methodological approaches exist to characterise uncertainty in geothermal Organic Rankine Cycle (ORC) projects, including Volumetric Monte Carlo Analysis, Sensitivity and Tornado Diagrams, Probabilistic Reservoir Modelling, and Case Study Evaluation [63,64]. Empirical studies of real-world U.S. geothermal installations—drawing on market data and dispatch behaviour—highlight the strategic value of flexible operation. Modes such as curtailment during negative pricing and ramp-up during high-price periods can increase the value of geothermal electricity generation by $1–$4/MWh [63]. Such a value range underscores the importance of staged or adaptive development strategies, particularly in the face of subsurface uncertainty or underperformance. In the case of the Zharkunak field, however, available data are currently limited to surface-level temperature and water composition, precluding detailed resource characterisation at this stage.

To address this limitation while ensuring realistic performance forecasting, a probabilistic assessment was conducted for the three geothermal wells analysed in this study. Seasonal operational modelling was complemented by a Monte Carlo simulation with 10,000 iterations, applying $a \pm 10$ % standard deviation around the median (P50) thermal output to capture plausible variability in geothermal system performance (Fig. 9). This uncertainty band is supported by published research: Steinbach et al. (2021) report an 8–12 % variation in thermal output due to borehole placement and subsurface heterogeneity in closed-loop systems [69], while Miranda et al. (2020) identify a 10–15 % spread between P10 and P90 values in deep geothermal reservoirs caused by geological and operational variability [70]. These findings validate the adopted uncertainty range and justify its application in risk-adjusted energy yield projections for ORC-based geothermal electricity generation in Kazakhstan.

For Well 5539, operating at a geothermal input of 376.2 K with 90 % annual availability, the estimated electricity output is 5 467.0 GWh/year (P50). The conservative P90 scenario yields 4 920.3 GWh/year, while the optimistic P10 scenario reaches 6 013.7 GWh/year. Well 1-RT, with an input of 371.2 K, shows a median production of 2 471.3 GWh/year, bounded by 2 224.2 GWh (P90) and 2 718.4 GWh (P10). Well 2-TP, operating at 360.4 K, delivers 2 597.9 GWh/year (P50), with the range extending from 2 338.1 GWh (P90) to 2 857.7 GWh (P10).

Based on international benchmarks, the levelized cost of electricity (LCOE) for shallow closed-loop geothermal systems ranges between USD $56 and $102 per MWh, with a representative P50 value of around $70/MWh [71]. Applying this distribution to the three wells analysed, Well 5539, with a median annual production of 5 467 GWh, results in a P50 cost of $0.070/kWh, bounded by a conservative P90 estimate of $0.090/kWh and an optimistic P10 of $0.055/kWh. Wells 1-RT and 2-TP, despite their lower output levels, fall within the same cost range due to similar operational parameters and thermal conditions.

The estimated LCOE for these geothermal wells ranges from $0.055/kWh (P10, optimistic case) to $0.090/kWh (P90, conservative case), with a median (P50) of $0.070/kWh. While the actual production costs of coal-fired power plants are often undisclosed due to market regulation and proprietary accounting, international benchmarks suggest that, under high-efficiency and strong pollution-control scenarios, coal-generated electricity typically falls between $0.065 and $0.095/kWh [72,73]. This indicates that in optimistic geothermal scenarios, electricity can be supplied at costs lower than those of advanced coal plants with full emission controls. Even in conservative scenarios, geothermal LCOE remains within the same range while providing significantly lower carbon intensity and minimal air pollution.

These values account for seasonal load changes and uncertainties in thermal performance, providing decision-makers with a probabilistic framework that improves the resilience of operational and investment planning. As site-specific knowledge advances and subsurface conditions are better characterised, these uncertainty bands are expected to narrow. This study is the first to assess the energy yield and costs of geothermal electricity generation using Organic Rankine Cycle (ORC) systems in this context, establishing a foundational benchmark for future technical improvements and economic evaluations.

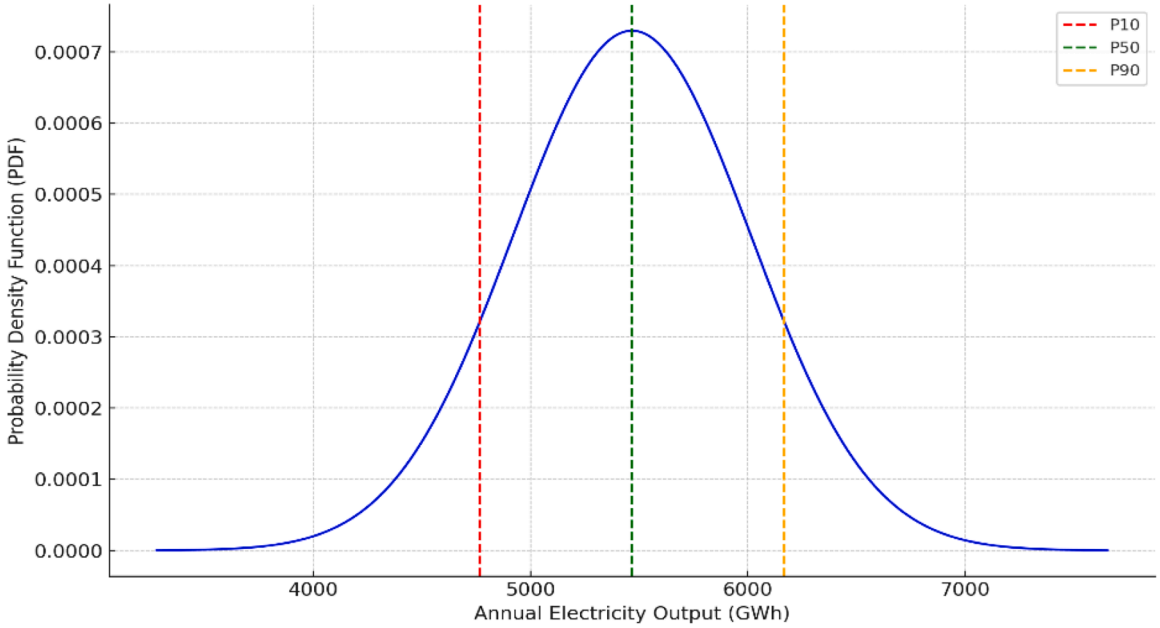

Fig. 9. Probability Density Function of the Annual Electricity Output for Well 5539 with the representation of P10, P50, and P90 uncertainties, for $a \pm 10$ % standard deviation around the median (P50) in a Monte Carlo simulation with 10,000 iterations.

5. Conclusions

This study offers the first comprehensive techno-economic and uncertainty assessment of geothermal electricity generation using Organic Rankine Cycle (ORC) technology in Kazakhstan. A territorial mapping of geothermal resources was conducted using QGIS 3.32.0, identifying significant potential in the Almaty and Mangystau regions. In particular, the Zharkunak field in the Almaty region stands out for its high-temperature wells—most notably well 5539—with an estimated annual electricity output of 5 467.0 GWh, accounting for 51.9 % of the region's geothermal potential. This output could offset up to 5.47 million tonnes of CO_2 emissions annually. The total potential production from wells in the Zharkent basin reaches 10.5 TWh/year, sufficient to cover 82.1 % of the region's electricity deficit.

Thermal performance modelling confirmed the technical feasibility of ORC deployment. Well 5539 achieved a calculated cycle efficiency of 11.86 %, aligning with the international benchmark range of 8–12 % for low-enthalpy binary systems. This supports the model's credibility and the suitability of ORC systems under Kazakhstan's geothermal conditions.

In terms of emission mitigation, replacing coal-fired electricity with geothermal energy from Zharkent could reduce annual CO_2 emissions by up to 10.54 million tonnes, based on standard emission factors.

A thermodynamic screening of 14 working fluids identified R-152a as the optimal candidate, combining high thermal efficiency, low global warming potential, and favourable operational properties.

Uncertainty in electricity generation was addressed through a Monte Carlo simulation incorporating $a \pm 10$ % standard deviation. For Well 5539, the projected electricity output ranged from 4 920.3 GWh (P90) to 6 013.7 GWh (P10), with a median of 5 467.0 GWh (P50).

The uncertainty analysis was complemented by a levelised cost of electricity (LCOE) analysis, which returned a range of $0.055–$0.090/kWh and a median estimate of $0.070/kWh. These figures confirm the economic competitiveness of geothermal energy, especially in light of its environmental advantages over fossil-based generation.

Limitations of this study include the absence of direct wellhead pressure and flow rate data, which necessitated the use of conservative assumptions based on geological inference. Nonetheless, the results establish a robust scientific foundation for geothermal development in Kazakhstan and provide a practical reference for energy planning and policy design. At the same time, the analysis demonstrates the technical viability, environmental value, and economic attractiveness of ORC-based geothermal energy—particularly in the Almaty region—as a strategic pillar for diversifying and decarbonising the national energy system.

Kazakhstan's geothermal potential remains largely untapped. The findings indicate that geothermal resources in Central Asia, which have long been overlooked in regional energy analyses, can play a significant role in mitigating electricity deficits and reducing CO_2 emissions. ORC technology thus emerges as a credible complement to Kazakhstan's coal-dominated electricity mix, with the potential to strengthen both energy security and decarbonisation pathways.

Future research should build upon the current modelling by including site-specific reservoir simulation, dynamic load matching, and assessment of long-term operational reliability under local geochemical conditions. Pilot-scale demonstration projects in the Almaty and Mangystau-Ustyurt basins would be especially beneficial to verify the modelled efficiencies and techno-economic estimates. Additionally, a comparative analysis with alternative renewable technologies within Kazakhstan's policy framework would help to further clarify the role of geothermal energy in the country's national energy transition.

Funding

This research has been funded by the Science Committee of the Ministry of Education and Science of the Republic of Kazakhstan (Grant №. BR24992867).

CRediT authorship contribution statement

Nazym Abdlakhatova: Writing – review & editing, Writing – original draft, Resources, Methodology, Formal analysis, Conceptualization. **Luis Frölén Ribeiro:** Writing – review & editing, Writing – original draft, Validation, Supervision, Methodology, Formal analysis, Data curation, Conceptualization. **Larysa Savosh:** Writing – review & editing, Writing – original draft, Methodology, Formal analysis, Data curation, Conceptualization. **Seitzhan Orynbayev:** Validation, Supervision, Software, Funding acquisition, Conceptualization. **Amanzhol**

Tokmoldayev: Supervision, Software. **Talgat Zhussip:** Software, Resources.

Declaration of competing interest

The authors declare that they have no known competing financial interests or personal relationships that could have appeared to influence the work reported in this paper.

Data availability statement

The original contributions presented in the study are included in the article, further inquiries can be directed to the corresponding author.

Data availability

Data will be made available on request.

References

[1] L.C.A. Gutiérrez-Negrín, Evolution of worldwide geothermal power 2020–2023, Geotherm. Energy 12 (2024) 14, https://doi.org/10.1186/s40517-024-00290-w.

[2] International Energy Agency (IEA), Versailles Statement: The crucial Decade for Energy Efficiency, IEA, 2023 [Online]. Available: https://www.iea.org/news/versailles-statement-the-crucial-decade-for-energy-efficiency.

[3] International Energy Agency (IEA), 8th Annual Global Conference on Energy Efficiency, IEA, 2023 [Online]. Available: https://www.iea.org/events/8th-annual-global-conference-on-energy-efficiency.

[4] J.S.C. Samruk-Energy, Obzor rynka elektroenergii i uglya Kazakhstana. Strategicheskii otchet AO Samruk-Energy za 2021 god [Overview of the electricity and coal market in Kazakhstan. Samruk-Energy's strategic report for 2021], Russian, Samruk-Energy [Online]. Available: https://www.samruk-energy.kz/images/documents/SamrukEnergy_AR-2021_RU.pdf, 2022.

[5] J.S.C. Samruk-Energy, Obzor rynka elektroenergii i uglya Kazakhstana. Strategicheskii otchet AO Samruk-Energy za 2014 god [Overview of the electricity and coal market in Kazakhstan. Samruk-Energy's strategic report for 2014], Russian, Samruk-Energy [Online]. Available, https://ar2014.samruk-energy.kz/upload/en/pdf/Annual_Report_2014.pdf, 2015.

[6] Government of the Republic of Kazakhstan, ob utverzhdenii kontseptsii razvitiia toplivno-energeticheskogo kompleksa Respubliki Kazakhstan na 2023–2029 gody [On approval of the Concept of Development of Fuel and Energy Complex of the Republic of Kazakhstan for 2023–2029], Russian, Postanovlenie No. 724, Gov. Rep. Kazakhstan (2023) [Online]. Available, https://adilet.zan.kz/rus/docs/P1400000724.

[7] KEGOC, Production and consumption of electricity in Kazakhstan in 2023, KEGOC (2023) [Online]. Available, https://www.kegoc.kz/kegoc_2023_rus.pdf.

[8] A. Kozhagulova, et al., Low salinity upper cretaceous formation potential for geothermal energy harvesting in the Eastern Ily Basin, Kazakhstan, in: EAGE GET Conf. Proc, Nov. 2022, pp. 1–5, https://doi.org/10.3997/2214-4609.202221052.

[9] A.M. Baikadamova, The use of geothermal energy using the example of the Zharkent geothermal water deposit, Eng. J. Satbayev Univ. 146 (4) (2024) 41–46, https://doi.org/10.51301/ejsu.2024.i4.06.

[10] R. Kutzhanov, Geothermal Assessment of a Depleted Naturally Fractured Reservoir in Zharkent Basin: A review, Master's thesis, Nazarbayev University, Nur-Sultan, 2022 [Online]. Available: http://nur.nu.edu.kz/handle/123456789/6552.

[11] QAZAQ GREEN, Development of renewable energy sources, Qazaqgreen.com (2022) [Online]. Available, https://qazaqgreen.com.

[12] J. Sagin, D. Adenova, A. Tolepbayeva, V. Poryadin, Underground water resources in Kazakhstan, Int. J. Environ. Stud. 74 (3) (2017) 386–398, https://doi.org/10.1080/00207233.2017.1288059.

[13] Natsional'nyi atlas Respubliki Kazakhstan. Prirodnye usloviia i resursy [National Atlas of the Republic of Kazakhstan. Natural conditions and resources], Russian, Vol. 1, Almaty (2010). ISBN 9786017150075.

[14] A.E. Ciriaco, S.J. Zarrouk, G. Zakeri, Geothermal resource and reserve assessment methodology: overview, analysis and future directions, Renew. Sustain. Energy Rev. (2019), https://doi.org/10.1016/j.rser.2019.109515.

[15] S. Umran, E.M. Cobanoglu, K. Didem, D. Zulfu, K. Gizem, Assessment of geothermal power potential in the Gediz Basin, Turkey, geothermics, 2022. https://doi.org/10.1016/j.geothermics.2022.102495.

[16] Y. Yerdesh, T. Amanzholov, A. Aliuly, A. Seitov, A. Toleukhanov, M. Murugesan, et al., Experimental and theoretical investigations of a ground source heat pump system for water and space heating applications in Kazakhstan, Energies. (Basel) 15 (22) (2022) 8336, https://doi.org/10.3390/en15228336.

[17] A. Kozhagulova, S. Makhambet, S. Tillabaev, D. Nurgaliyev, Geothermal energy potential of the Mangyshlak Basin, western Kazakhstan: a preliminary assessment based on stratigraphy and temperature data, Geothermics. 109 (2023) 102655, https://doi.org/10.1016/j.geothermics.2023.102655.

[18] A. Kozhagulova, S. Makhambet, S. Tillabaev, D. Nurgaliyev, A preliminary assessment of geothermal energy potential of Mangyshlak sedimentary basin in Kazakhstan, EAGE GET Conf. Proc. (2021), https://doi.org/10.3997/2214-4609.202121029.

[19] Kazakhstan Electricity Grid Operating Company (KEGOC), Almatinskiye MES: overhead transmission lines 0.4–500 kV (4219.61 km) and 12 substations 35–500 kV with total transformer capacity of 4958.2 MVA, KEGOC (2025) [Online]. Available: https://www.kegoc.kz/en.

[20] Z. Wu, D. Pan, N. Gao, T. Zhu, F. Xie, Experimental testing and numerical simulation of scroll expander in a small-scale Organic Rankine Cycle system, Appl. Therm. Eng. 87 (2015) 529–537, https://doi.org/10.1016/j.applthermaleng.2015.05.040.

[21] C. Zhang, J.L. Fu, P.F. Yuan, J.J. Liu, Guidelines for optimal selection of subcritical low-temperature geothermal Organic Rankine cycle configuration considering reinjection temperature limits, Energies. (Basel) 11 (2018) 2878, https://doi.org/10.3390/en11112878.

[22] Z. Guzović, Z. Bačelić Medić, M. Budanko, Effect of working fluid on characteristics of organic rankine cycle with medium temperature geothermal water, Energies. (Basel) 18 (7) (2025) 1699. https://www.mdpi.com/1996-1073/18/7/1699.

[23] T. Hai, A.S. El-Shafay, A. Alizadeh, B.S. Chauhan, Combination of a geothermal-driven double-flash cycle and a Kalina cycle for power generation and emission reduction, Appl. Therm. Eng. 223 (2023) 115055, https://doi.org/10.1016/j.applthermaleng.2022.115055.

[24] M. Kaczmarczyk, B. Tomaszewska, L. Pająk, Geological and thermodynamic analysis of a binary cycle power plant for geothermal water in Poland, Energies. (Basel) 13 (6) (2020) 1335, https://doi.org/10.3390/en13061335.

[25] H. Li, D. Hu, M. Wang, Y. Dai, Off-design performance analysis of a Kalina cycle for geothermal fields with seasonal output, Appl. Therm. Eng. 107 (2016) 447–456, https://doi.org/10.1016/j.applthermaleng.2016.06.120.

[26] C. Öksel, A. Koç, Modeling of a combined Kalina and Organic Rankine Cycle system for waste heat recovery from a biogas engine, Sustainability. 14 (12) (2022) 7135, https://doi.org/10.3390/su14127135.

[27] A. Shokri Kalan, H. Ghiasirad, R. Khoshbakhti Saray, S. Mirmasoumi, Thermo-economic evaluation and multi-objective optimization of a waste heat driven combined cooling and power system based on a modified Kalina cycle, Energy Convers. Manage 247 (2021) 114723, https://doi.org/10.1016/j.enconman.2021.114723.

[28] C. Penot, D. Martelo, S. Paul, Corrosion and scaling in geothermal heat exchangers, Appl. Sci. 13 (20) (2023) 11549, https://doi.org/10.3390/app132011549.

[29] V. Salnikov, G. Turulina, S. Polyakova, Y. Petrova, A. Skakova, Climate change in Kazakhstan during the past 70 years, Quat. Int. (2014), https://doi.org/10.1016/j.quaint.2014.09.008.

[30] W.G. Vincenti, Control-volume analysis: a difference in thinking between engineering and physics, Technol. Cult. 23 (2) (1982) 145–174, https://doi.org/10.2307/3104129.

[31] H.A. Sorensen, Principles of Thermodynamics, Holt, Rinehart and Winston, New York, 1961.

[32] Y.A. Çengel, Thermodynamics: An Engineering Approach, McGraw-Hill Higher Education, Boston, 2008 eBook ISBN: 9780077366742.

[33] M. Astolfi, M.C. Romano, P. Bombarda, E. Macchi, Binary ORC (organic Rankine cycles) power plants for the exploitation of medium–low temperature geothermal sources – Part B: techno-economic optimization, Energy 66 (2014) 435–446, https://doi.org/10.1016/j.energy.2013.11.077.

[34] X. Yu, J. Geng, Z. Gao, Thermal-economic analysis of an organic Rankine cycle system with direct evaporative condenser, J. Adv. Therm. Sci. Res. 10 (4) (2023), https://doi.org/10.15377/2409-5826.2023.10.4.

[35] J.M. Chicco, G. Madrone, How a sensitive analysis on the coupling geology and borehole heat exchanger characteristics can improve the efficiency and production of shallow geothermal plants, Heliyon. 26 (2022), https://doi.org/10.1016/j.heliyon.2022.e09545.

[36] R. Tonkin, J. O'Sullivan, M. Gravatt, M. O'Sullivan, A transient geothermal wellbore simulator, Geothermics. 110 (2023) 102653, https://doi.org/10.1016/j.geothermics.2023.102653.

[37] C. Chen, H. Zhou, T. Nagel, et al., Parametric analysis on the transient two-phase wellbore model applied to the Yangyi high-temperature geothermal field, Geotherm. Energy 13 (1) (2025) 1, https://doi.org/10.1186/s40517-024-00322-5.

[38] I.H. Bell, J. Wronski, J. Quoilin, S. Quoilin, L. Vincent, Pure and pseudo-pure fluid thermophysical property evaluation and the open-source thermophysical property library CoolProp, Ind. Eng. Chem. Res. 53 (6) (2014) 2498–2508. http://pubs.acs.org/doi/abs/10.1021/ie4033999.

[39] A.M. Jubori, F.N. Al Mousawi, K. Rahbar, R. Al Dadah, S. Mahmoud, Design and manufacturing a small-scale radial inflow turbine for clean organic Rankine power system, J. Clean. Prod. 254 (2020) 120488, https://doi.org/10.1016/j.jclepro.2020.120488.

[40] M. Imran, M. Usman, B.S. Park, D.H. Lee, Volumetric expanders for low grade heat and waste heat recovery applications, Renew. Sustain. Energy Rev. 57 (2016) 1090–1109, https://doi.org/10.1016/j.rser.2015.12.139.

[41] J. Niu, J. Wang, X. Liu, Thermodynamic and economic analysis of organic rankine cycle combined with flash cycle and ejector, Energy 282 (2023) 128982, https://doi.org/10.1016/j.energy.2023.128982.

[42] H. Florian, D. Dieter, Thermo-economic evaluation of organic Rankine cycles for geothermal power generation using zeotropic mixtures, Energies. (Basel) 8 (3) (2015) 2097–2124, https://doi.org/10.3390/en8032097.

[43] X. Huan, et al., A graphical criterion for working fluid selection and thermodynamic system comparison in waste heat recovery, Appl. Therm. Eng. 89 (2015) 772–782, https://doi.org/10.1016/j.applthermaleng.2015.06.050.

[44] X.L. Luo, et al., Improved correlations for working fluid properties prediction and their application in performance evaluation of sub-critical organic rankine cycle, Energy 174 (2019) 122–137, https://doi.org/10.3390/min12030280.
[45] Q. Liu, R. Chen, X. Yang, X. Xiao, Thermodynamic analyses of sub and supercritical ORCs using R1234yf, R236ea and their mixtures as working fluids for geothermal power generation, Energies. (Basel) 16 (2023) 5676, https://doi.org/10.3390/en16155676.
[46] V.Z. Geller, N.I. Lapardin, Solubility and miscibility of refrigerants R407c and R410A with synthetic compression oils, Odessa Natl. Acad. Food Technol., Odessa, Ukraine (2016), https://doi.org/10.15673/ret.v52i3.121.
[47] M. Ennio, A. Marco, Organic Rankine Cycle (ORC) Power Systems Technologies and Applications, 1st Edition, Elsevier, 2016. August 24eBook ISBN: 9780081005118, https://shop.elsevier.com/books/organic-rankine-cycle-orc-power-systems/macchi/978-0-08-100510-1.
[48] M. Shahpar, A. Hajinezhad, R. Fattahi, S.F. Moosavian, Efficient refrigerant strategies for large-scale geothermal heat pumps: triple analysis of energy, exergy, and cost, Results Eng. 26 (2025) 104052, https://doi.org/10.1016/j.rineng.2025.104052.
[49] M. Shalby, A. Marachli, A.A. Salah, Working fluid selection and performance analysis for subcritical organic rankine cycles, Results. Eng. 25 (2025) 104120, https://doi.org/10.1016/j.rineng.2025.104120.
[50] B.K. Saha, E.M.B. Messini, P. Kumar, Addressing industrial waste heat supply variability with Organic Rankine Cycle systems incorporating thermal energy storage, Results. Eng. 25 (2025) 103768, https://doi.org/10.1016/j.rineng.2024.103768.
[51] Technical University of Denmark (DTU), CoolPack: A collection of Simulation Tools For Refrigeration, DTU, 2000 [Online]. Available: https://www.ipu.dk/products/coolpack/.
[52] Pyromat: a Python library for thermodynamic calculations, Pyromat (2025) [Online]. Available, http://pyromat.org/live/.
[53] Thermostate: thermodynamics state software, Thermostate (2025) [Online]. Available: https://thermo-state.github.io.
[54] United Nations Environment Programme (UNEP), Kigali Amendment to the Montreal Protocol on Substances that Deplete the Ozone Layer, UNEP, Nairobi, 2016 [Online]. Available, https://ozone.unep.org/treaties/montreal-protocol/amendments/kigali-amendment-20.
[55] ASHRAE, Standard 34: Designation and Safety Classification of Refrigerants, American Society of Heating, Refrigerating and Air-Conditioning Engineers, Atlanta, GA, 2013 [Online]. Available: https://www.ashrae.org/technical-resources/bookstore/standard-34.
[56] S. Kondo, K. Takizawa, K. Tokuhashi, Flammability limits of binary mixtures of ammonia with HFO-1234yf, HFO-1234ze, HFC-134a, and HFC-125, J. Fluor. Chem. 149 (2) (2023) 18–23, https://doi.org/10.1016/j.jfluchem.2013.02.010.
[57] ASHRAE, Standard 34-2022: Designation and Safety Classification of Refrigerants, American Society of Heating, Refrigerating and Air-Conditioning Engineers, Atlanta, GA, 2022 [Online]. Available: https://www.ashrae.org/technical-resources/standards-and-guidelines/standards-addenda.
[58] C. Arpagaus, M. Uhlmann, F. Bless, High-temperature ORC systems using flammable working fluids: safety and performance, Energy Rep. 9 (2023) 435–445, https://doi.org/10.1016/j.egyr.2023.01.007.
[59] S. Wieland, M. Gölles, T. Schitthelm, D. Brüggemann, Material compatibility of ORC working fluids with polymers, Energy 103 (2016) 660–671, https://doi.org/10.1016/j.energy.2016.02.127.
[60] Samruk-Energy, Overview of the electricity and coal market in Kazakhstan, Samruk-Energy (2023) [Online]. Available: https://ar2023.samruk-energy.kz/ru/overview-of-the-electricity-and-coal-market-in-kazakhstan.html.
[61] Transmark Renewables, Kaishan, Transmark Renewables and Kaishan form JV for expansion of Gülpınar geothermal project, Turkiye, Think Geo. Energy (2022) [Online]. Available: https://www.thinkgeoenergy.com/transmark-renewables-and-kaishan-form-jv-for-expansion-of-gulpinar-geothermal-project-turkiye.
[62] G.V. Tomarov, A.A. Shipkov, Multistage organic rankine cycles: utilization of medium temperature (120 °C) geothermal fluid, Therm. Eng. 69 (2022) 354–361, https://doi.org/10.1134/S0040601522050068.
[63] D. Millstein, P. Dobson, S. Jeong, The potential to improve the value of U.S. geothermal electricity generation through flexible operations, J. Energy Resour. Technol. 143 (1) (2021) 011005, https://doi.org/10.1115/1.4048981.
[64] C. Augustine, K.F. Beckers, K. Young, A. Anderson, Geothermal Resource Portfolio Optimization and Assessment: Incorporating Uncertainty and Technical Risk, NREL, Golden, CO, 2019 [Online]. Available: https://www.nrel.gov.
[65] S.K. Sanyal, Cost of geothermal power and factors that affect it, Proc. Geothermal Energy Council annu. Meet., Palm Springs, CA (2004).
[66] A. Franco, M. Villani, Optimal design of binary cycle power plants for water-dominated, medium-temperature geothermal fields, Geothermics. 38 (4) (2009) 379–391, https://doi.org/10.1016/j.geothermics.2009.08.001.
[67] IEA-RETD, Risk Mitigation Instruments for Renewable Energy Projects: Summary of Findings, IEA-RETD, 2015 [Online]. Available, https://iea-retd.org/documents.
[68] P. Akto, Z. Chen, K. Hu, Evaluation of geothermal resource potential of hot sedimentary aquifers in the Horn River Basin, northeast British Columbia, Canada, Geol. Surv. Can., Open File 8939 (2023) 38, https://doi.org/10.4095/331225.
[69] P. Steinbach, D.O. Schulte, B. Welsch, I. Sass, J. Lang, Quantification of bore path uncertainty in borehole heat exchanger arrays using adaptive anisotropic stochastic collocation, Geothermics. 97 (2021) 102194, https://doi.org/10.1016/j.geothermics.2021.102194.
[70] M.M. Miranda, J. Raymond, C. Dezayes, Uncertainty and risk evaluation of deep geothermal energy source for heat production and electricity generation in remote northern regions, Energies. (Basel) 13 (16) (2020) 4221, https://doi.org/10.3390/en13164221.
[71] International Renewable Energy Agency (IRENA), Renewable Power Generation Costs in 2020, IRENA, Abu Dhabi, 2021 [Online]. Available, https://www.irena.org/publications/2021/Jun/Renewable-Power-Costs-in-2020.
[72] International Energy Agency (IEA), Nuclear Energy Agency (NEA), Projected Costs of Generating Electricity 2020, OECD Publishing, Paris, 2021 [Online]. Available, https://www.iea.org/reports/projected-costs-of-generating-electricity-2020.
[73] World Bank, Global Electricity Prices and Generation Cost Database, EnergyData.Info [Online]. Available, https://energydata.info, 2022.